Article

Energy and Electron Transfer in Enhanced Two-Photon-Absorbing Systems with Triplet Cores

Olga S. Finikova, Thomas Troxler, Alessandro Senes, William F. DeGrado, Robin M. Hochstrasser, and Sergei A. Vinogradov

More About This Article

Additional resources and features associated with this article are available within the HTML version:

- Supporting Information
- Links to the 7 articles that cite this article, as of the time of this article download
- Access to high resolution figures
- Links to articles and content related to this article
- Copyright permission to reproduce figures and/or text from this article

View the Full Text HTML

Energy and Electron Transfer in Enhanced Two-Photon-Absorbing Systems with Triplet Cores

Olga S. Finikova,[†] **Thomas Troxler,**[‡] **Alessandro Senes,**[†] **William F. DeGrado,**[†]
Robin M. Hochstrasser,[‡] **and Sergei A. Vinogradov*,**[†]

Departments of Biochemistry and Biophysics and Chemistry, University of Pennsylvania, Philadelphia, Pennsylvania 19104

Enhanced two-photon-absorbing (2PA) systems with triplet cores are currently under scrutiny for several biomedical applications, including photodynamic therapy (PDT) and two-photon microscopy of oxygen. The performance of so far developed molecules, however, is substantially below expected. In this study we take a detailed look at the processes occurring in these systems and propose ways to improve their performance. We focus on the interchromophore distance tuning as a means for optimization of two-photon sensors for oxygen. In these constructs, energy transfer from several 2PA chromophores is used to enhance the effective 2PA cross section of phosphorescent metalloporphyrins. Previous studies have indicated that intramolecular electron transfer (ET) can act as an effective quencher of phosphorescence, decreasing the overall sensor efficiency. We studied the interplay between 2PA, energy transfer, electron transfer, and phosphorescence emission using Rhodamine B–Pt tetrabenzoporphyrin (RhB–PtTBP) adducts as model compounds. 2PA cross sections (σ_2) of tetrabenzoporphyrins (TBPs) are in the range of several tens of GM units (near 800 nm), making TBPs superior 2PA chromophores compared to regular porphyrins (σ_2 values typically 1–2 GM). Relatively large 2PA cross sections of rhodamines (about 200 GM in 800–850 nm range) and their high photostabilities make them good candidates as 2PA antennae. Fluorescence of Rhodamine B (λ_{fl} = 590 nm, ϕ_{fl} = 0.5 in EtOH) overlaps with the Q-band of phosphorescent PtTBP (λ_{abs} = 615 nm, ϵ = 98 000 M^{-1} cm^{-1}, $\phi_p \sim$ 0.1), suggesting that a significant amplification of the 2PA-induced phosphorescence via fluorescence resonance energy transfer (FRET) might occur. However, most of the excitation energy in RhB–PtTBP assemblies is consumed in several intramolecular ET processes. By installing rigid nonconducting decaproline spacers (Pro$_{10}$) between RhB and PtTBP, the intramolecular ETs were suppressed, while the chromophores were kept within the Förster r_0 distance in order to maintain high FRET efficiency. The resulting assemblies exhibit linear amplification of their 2PA-induced phosphorescence upon increase in the number of 2PA antenna chromophores and show high oxygen sensitivity. We also have found that PtTBPs possess unexpectedly strong forbidden S$_0$ → T$_1$ bands (λ_{max} = 762 nm, ϵ = 120 M^{-1} cm^{-1}). The latter may overlap with the laser spectrum and lead to unwanted linear excitation.

Introduction

Two-photon laser scanning microscopy (2P LSM), pioneered by Denk and Webb in 1990,[2] has become one of the most popular tools in modern neuroscience and cellular research.[3] 2P LSM is based on the multiphoton-absorption phenomenon,[4] which presents considerable interest for such applications as high-density data storage,[5] optical limiting,[6] and photodynamic therapy (PDT),[7] attracting more and more chemists to the search for new multiphoton-absorbing materials. Typically, two-photon-absorption (2PA) cross sections (σ_2)[1] of commonly used organic dyes are small and only in a few cases (e.g., rhodamines) reach moderate values, e.g., hundreds of Göppert-Mayer (GM) units.[8] A number of systems with enhanced 2PA cross sections have been proposed in recent years,[9–14] and rational ways of designing 2PA molecules are being developed.[9a,15]

Although large σ_2 values are generally desirable for all 2PA optical probes, imaging with fluorescent agents, which typically possess high quantum yields, can be accomplished even when they exhibit low 2PA cross sections. On the contrary, for emitters with intrinsically low quantum yields and/or long excited-state lifetimes, such as phosphorescent probes, amplification of 2PA is an absolute requirement. Phosphorescent probes are useful for biological measurements because their long lifetimes make them extremely sensitive to a variety of quenching processes. One such process involves oxygen—a key component of the biological energy metabolism. Oxygen sensing in vivo by phosphorescence[16,17] is a technology with many potential uses in physiological and medical research,[18] including applications in microscopy and imaging.[19] Combining phosphorescence quenching with 2P LSM would provide a new technique for high-resolution imaging of oxygen with intrinsic three-dimensional capability—a useful tool for studying neuronal activation, evaluating heterogeneity of hypoxia in tumors, and monitoring metabolic processes inside living cells.

Phosphorescent probes for biological oxygen sensing are usually based on Pd or Pt porphyrins, whose intersystem crossing rates and phosphorescence quantum yields are high and whose submillisecond triplet lifetimes ensure their excellent

* Corresponding author. E-mail: vinograd@mail.med.upenn.edu.
† Department of Biochemistry and Biophysics.
‡ Department of Chemistry.

oxygen sensitivity.[20] Unfortunately, 2PA cross sections of metalloporphyrins and other useful phosphorescent dyes, such as $Ru^{2+}(bpy)_3$ and similar complexes,[17] are typically very low, no more than several GM units.[21,22] In centrosymmetrical molecules, selection rules for one-photon (1P) and 2P transitions are mutually exclusive, and excited states corresponding to the strongly allowed Soret and Q-band transitions of metalloporphyrins have correspondingly weak 2PA cross sections.[23] Recently, much attention has been focused on tetrapyrroles with increased 2PA cross sections. 2PA of porphyrins can be increased by asymmetrical substitution[24] or through porphyrin conjugation into oligomers and arrays.[10] Some of these new materials appear to be effective in singlet oxygen sensitization; however, no explicit data have been reported on their triplet quantum yields. Similarly, no data on phosphorescence of 2PA porphyrins have been published, and it is not clear how perturbation of the porphyrin electronic system would affect the emissivity of its triplet states. In addition, some data suggest that increase in the length of porphyrin arrays causes a decrease in their intersystem crossing yields and hampers triplet production.[25]

An alternative approach to amplification of 2PA signals from porphyrins without directly altering their electronic properties has recently been proposed as a means of constructing phosphorescent oxygen sensors[26] and 2PA PDT agents.[27] The idea behind this approach is to harvest the excitation energy by an electronically separate 2PA antenna, which then would pass the excitation to the porphyrin via intramolecular Förster-type resonance energy transfer (FRET).[28] Intersystem crossing (isc) within the porphyrin then generates the triplet state, which decays back to the ground state by either emitting a photon (phosphorescence) or sensitizing oxygen. In phosphorescent sensors, the rate of oxygen diffusion to the core is regulated by dendritic encapsulation, while the dendrimer termini control the probe's biodistribution.[18e,29] Several model compounds have been constructed in order to evaluate this design, proving that the approach is feasible and promising. However, certain difficulties have been identified as well.

First of all, amplification of the core function—whether it is emission or singlet oxygen sensitization—did not appear to scale linearly with the 2PA cross section of the antenna. Instead, structures with built-in enhancement pathways showed lower performance than theoretically expected from their estimated 2PA action cross sections. Second and more importantly, electron transfer (ET) between the antenna and the triplet-state core was identified as an unwanted but extremely effective route for the triplet quenching. Preventing the ET between the core and the 2PA antenna would either require chromophores incapable of electron exchange or, more realistically, placing the chromophores at such a distance from one another that the ET would be diminished, while the FRET would be maintained at its highest possible rate. Such distance tuning should be possible because of the difference in the rate dependences for the Förster-type energy transfer[30,31] and electron transfer.[32,33]

Positioning chromophores at optimal distances, carefully selected during the course of evolution, is the key to the outstanding performance of natural photosynthetic systems, which employ combinations of energy- and electron-transfer reactions for energy transduction and conservation.[34] Not surprisingly, these processes have been studied by many researchers using a variety of synthetic models, and the literature covering this subject is very extensive.[32,35,36] In contrast, there are relatively few reports on the 2PA-induced FRET[27,37,38] and none, to our knowledge, on the combination of 2PA, FRET, and ET.

In this paper we studied model 2PA antenna−triplet core dyads to identify undesirable photoinduced ET processes and to evaluate their distance dependence. We then synthesized assemblies in which the antenna and the core were separated by nonconducting polyproline linkers at distances where the ETs were prevented but the energy transfer remained highly efficient. Finally, enhancement of the core 2PA-induced phosphorescence as a function of the number of antenna chromophores was measured in femtosecond regime. As a result, guidelines for design of optimized antenna−triplet core 2PA systems for biological applications were developed.

Results and Discussion

Functional Components of the Device. The first reported 2PA-amplified phosphorescent sensors consisted of Pt *meso*-tetraarylporphyrins (PtP) as triplet cores and commercial Coumarin-343 (C343) as 2PA antennae.[26] The FRET from C343 onto PtP was efficient (∼80%), and upon femtosecond (fs) excitation in the region of 800 nm an increase in the core phosphorescence was readily observed. However, amplification in 2PA-induced phosphorescence for all PtP−C343 systems was modest, in part due to the relatively low 2PA cross section of C343 ($\sigma_2 \sim 20$ GM).

In this study we turned our attention to rhodamines, which have 2PA cross sections of about 200 GM in the 840 nm range[8a,39] and potentially can perform as effective 2PA antennae. Rhodamine B (RhB, Figure 1) fluoresces near $\lambda_{max} \approx 590$ nm with the quantum yield $\phi_{fl} = 0.5$[40,41] and is known for its high photostability. Functionalized derivatives of RhB are readily accessible via the recently reported chemistry.[42]

To match the emission of RhB for the most efficient transfer of the excitation energy, we chose Pt *meso*-tetraaryltetrabenzoporphyrins (PtTBP, Figure 1) to be the triplet cores. Pt and Pd tetrabenzoporphyrins exhibit strong phosphorescence at ambient temperatures,[20d,43] and their NIR absorption bands warrant their use as probes for in vivo oxygen imaging.[19c,d,29c] A versatile method of synthesis of π-extended porphyrins has recently been developed,[44] making it possible to place various functional groups on the TBP macrocycle. The absorption Q-band of PtTBP **2** ($\lambda_{max} = 615$ nm, $\epsilon = 98\,000$ M^{-1} cm^{-1}) overlaps significantly with the fluorescence of RhB (Figure 1), suggesting efficient FRET between these two molecules. Assuming random orientation of transition dipoles ($\kappa^2 = 2/3$) and a refractive index of 1.36 (EtOH), the Förster distance r_0 for the RhB−PtTBP pair was estimated to be 53 Å.[45]

An important property of *meso*-tetraaryltetrabenzoporphyrins, especially in the view of the present application, is their high nonplanarity. TBPs and their metal derivatives possess severely saddled structures.[44b,46] As a result, their ground-state wave functions lack centers of symmetry, and that should cause an increase in their 2PA cross sections. Some data in the literature indeed mention relatively large σ_2 values for TBPs, e.g., about 90 GM ($\lambda_{ex} = 800$ nm) for Zn *meso*-tetraaryltetrabenzoporphyrin.[21b] Interestingly, in spite of strong nonplanarity, TBPs and other π-extended porphyrins exhibit high emission quantum yields,[20d,29c,43,44] while other nonplanar porphyrins are practically nonemissive, as a result of enhanced internal conversion.[47]

RhB−PtTBP Adducts with Short Spacers. The simplest bichromophoric assemblies studied in this work were RhB−PtTBP adducts, in which the antenna (RhB) and the core
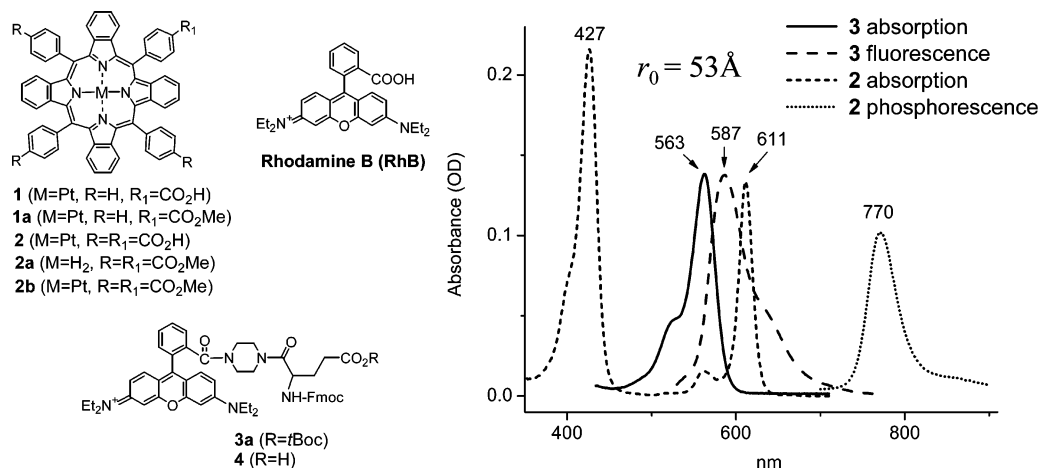
Two-Photon Oxygen Sensor

J. Phys. Chem. A, Vol. 111, No. 30, 2007 **6979**

Figure 1. (left) Functional components of the studied assemblies: *meso*-tetraaryltetrabenzoporphyrins (TBP, **1–2b**); Rhodamine B (RhB) and its functionalized derivatives (**3a** and **4**). (right) Absorption and emission spectra of PtTBP (**2**) and of **3a** in EtOH. For absorption spectra, the molar ratio of **2** and **3a** is 1:1. For emission, solution of **2** was purged with Ar; ordinate values are in arbitrary units.

TABLE 1: Photophysical Data for Compounds Described in This Paper[a]

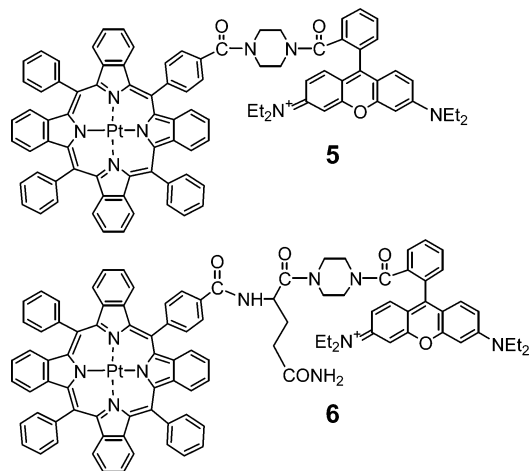| no.	solvent	λ_{abs}, nm (log ϵ)	λ_{em}, nm (λ_{ex}, nm), em type	ϕ[b]	ϕ_{FRET}	τ (lifetime)	σ_2,[c] GM
1a	DMF	614 (5.02)	772 (615), p	0.092	–	33 μs	(28)[d]
	EtOH	611 (5.02)	771 (615), p	0.083			
	CH$_2$Cl$_2$	614 (5.02)	774 (615), p	0.10			
2b	DMF	617 (5.03)	783 (615), p	0.074	–	31 μs	(28)[d]
3a	EtOH	563 (4.98)	587 (520), f	0.21	–	1.85 ns	200[e]
	DMF	565 (4.98)	588 (520), f	0.26			
	CH$_2$Cl$_2$	563 (4.98)	582 (520), f	0.33			
4	H$_2$O/EtOH, 1:1	566 (−)	587 (520), f	0.20	–	–	–
5	EtOH	563 (5.02)	770 (611), p	<0.001	0.21	<1 μs	–
		611 (5.02)	584 (520), f	0.004			
6	EtOH	563 (5.02)	770 (611), p	0.001	0.83	<1 μs	–
		611 (5.02)	584 (520), f	0.007			
7	DMF	565 (4.98)	587 (520), f	0.27	–	–	–
8	EtOH	563 (5.02)	770 (611), p	0.052	0.84	29 μs	224
		611 (5.02)	584 (520), f	0.028		0.33 ns	
	DMF	565 (5.02)	772 (611), p	0.052	0.84		
		614 (5.02)	588 (520), f	0.028			
	CH$_2$Cl$_2$	563 (5.02)	773 (611), p	0.035	0.84		
		613 (5.02)	580 (520), f	0.026			
9	DMF	565 (5.58)	776 (615), p	0.028	0.55	27 μs	(824)
		616 (5.03)	587 (520), f	0.043		0.44 ns	
10	BSA, 1% aq	646 (4.49)	668 (611), f	0.014	–	1.98 ns	28

[a] All measurements were performed in solvents deoxygenated by Ar bubbling. [b] Emission quantum yields were determined relative to the fluorescence of Rhodamine B in MeOH ($\phi_{fl} = 0.5$).[40] Measured against this value, *meso*-tetraphenylporphyrin (H$_2$TPP), a common standard for porphyrin spectroscopy, exhibits the absolute fluorescence quantum yield $\phi_{fl} = 0.048$ in deoxygenated benzene, as opposed to the generally accepted value $\phi_{fl} = 0.11$.[48,49] To transform the numbers in the table into the numbers relative to the quantum yield of H$_2$TPP ($\phi_{fl} = 0.11$), they should be multiplied by 2.29. [c] $\lambda_{ex} = 840$ nm, 110 fs, 76 MHz. [d] σ_2 values in parentheses are estimated (see text for details). [e] Reference 8a.

(PtTBP) were present in 1:1 ratio and connected via short nonconjugated linkers. Two such molecules, **5** and **6**, are shown in Scheme 1, and detailed description of their synthesis can be found in the Supporting Information.

Isolation and handling of **5** proved difficult. This compound degrades rapidly in concentrated solutions at ambient temperatures and decomposes, although slowly, even when shielded from ambient light. Pure **5** could be preserved by freezing its solutions immediately after chromatography. Adduct **6** turned out to be more stable than **5**, although its partial decomposition was revealed by the decrease in its RhB absorption when the compound was exposed to ambient light or handled at elevated temperatures.

A. Spectroscopy. The photophysical data for all the compounds described in this paper are summarized in Table 1. The absorption spectra of adducts **5** and **6** and of an equimolar mixture of reference compounds **1a** and **3a** are nearly identical, suggesting no interactions between the chromophores in their ground states (Figure 2A).

SCHEME 1: RhB−PtTBP Adducts with Short Spacers

The emission spectra shown in Figure 2B were recorded upon excitation at $\lambda_{ex} = 520$ nm, where the absorption of PtTBP is
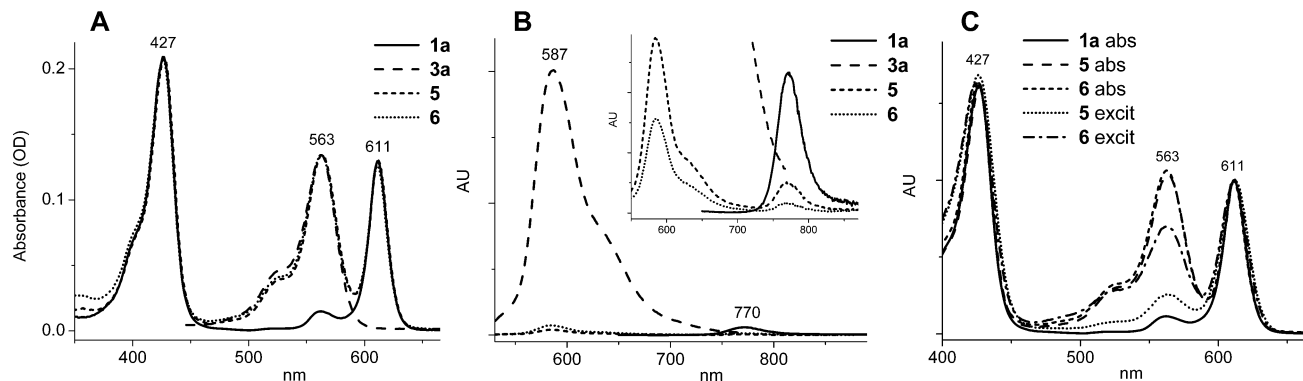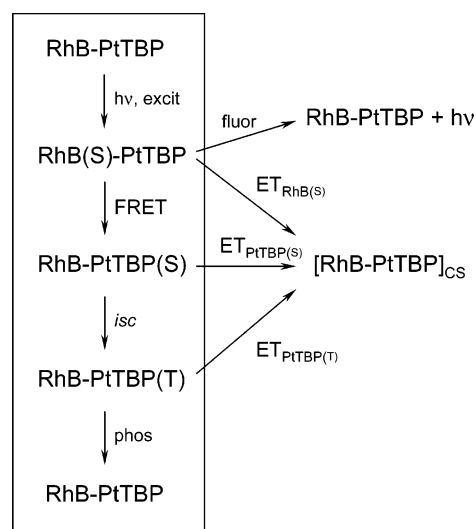
Figure 2. Absorption (A, C), emission (B), and excitation (C) spectra of adducts **5** and **6** and reference compounds **1a** and **3a** in EtOH. All measurements were performed in deoxygenated solutions. (A) Samples contain compounds in equal molar concentrations. (B) The emission spectra were normalized by the absorbance at $\lambda_{ex} = 520$ nm. Inset: enlarged graph. (C) Excitation spectra were recorded for $\lambda_{em} = 770$ nm.

low, whereas the absorption of RhB is significant. The intramolecular FRET between RhB and PtTBP in adducts **5** and **6** was expected to quench the fluorescence of RhB ($\lambda_{max} = 587$ nm), but at the same time amplify the phosphorescence of PtTBP ($\lambda_{max} = 770$ nm). Instead, both fluorescence and phosphorescence in **5** and **6** appeared to be almost entirely quenched (Figure 2B). Direct excitation into the porphyrin Q-band ($\lambda_{ex} = 611$ nm), bypassing the RhB absorption and the FRET, revealed that the phosphorescence quantum yields of **5** ($\phi_p < 0.001$) and **6** ($\phi_p = 0.001$) were decreased by 98–99% compared to the reference compound **1a** ($\phi_p = 0.083$ in EtOH). Quenching due to intermolecular aggregation was ruled out since the replacement of solvents (CH$_2$Cl$_2$, DMF) and/or dilution of samples (10–100 times) had almost no effect on the phosphorescence, and no evidence of aggregation was observed in the absorption spectra (Figure 2A). Such strong attenuation of the emission could be explained only by the presence of intramolecular quenching pathways in RhB–PtTBP adducts. The most plausible mechanisms would involve RhB ← PtTBP triplet–triplet energy transfer and intramolecular electron transfer(s) (ET), competing with the phosphorescence.

Both intramolecular and intermolecular ET between porphyrins and xanthene dyes have been described in the literature,[50] although, to the best of our knowledge, no studies involving phosphorescent porphyrins have been reported. On the other hand, literature data suggest that the T$_1$–S$_0$ gap for RhB is 1.86 eV (667 nm),[51] whereas phosphorescence of PtTBP occurs at 770 nm (1.61 eV), making RhB ← PtTBP triplet–triplet exchange energetically unfavorable. Thus, the ET between the excited PtTBP and RhB in its ground state is the most probable mechanism of the phosphorescence quenching. In principle, two such ETs are possible for RhB–PtTBP systems: one involving the PtTBP singlet state S$_1$ and competing with S$_1$ → T$_1$ intersystem crossing (isc) and another involving the PtTBP triplet state T$_1$ and competing with phosphorescence itself. Below, we refer to these ETs as ET$_{PtTBP(S)}$ and ET$_{PtTBP(T)}$, respectively.

Assuming the pure Förster model and the distance between the reactants of 13 Å,[52] the rate of the energy transfer in **5** was estimated to be $k_{FRET} = 2.5 \times 10^{12}$ s^{-1}.[45] At such a rate the residual emission from RhB, whose singlet-state lifetime in the absence of quenching is 1.85 ns (Table 1, **3a**), would be truly negligible. For example, in the case of **5**, the predicted quantum yield of RhB fluorescence is about 10^{-4}, whereas in our experiments it was 0.004 (Table 1, **5**). The observed discrepancy suggests that either rigid structural features are present in dyads **5** and **6**, which cause a major decrease in the value of the orientation factor κ^2, or contaminant fluorescence from an

SCHEME 2: Energy-/Electron-Transfer Pathways in RhB–PtTBP Adducts

impurity, e.g., unbound RhB, is the source of the increased apparent fluorescence quantum yield. The intensity of the contaminant fluorescence, however, is very small and does not affect our calculations (see below).

Energy-transfer efficiencies in **5** and **6** were estimated by comparing their excitation ($\lambda_{em} = 770$ nm) and absorption spectra (Figure 2C), scaled to the same value at the Q-band maximum ($\lambda_{ex} = 611$ nm).[53] In such measurements, an exact match between the absorption and excitation spectra would signify energy transfer with 100% efficiency. The intensities of the RhB bands ($\lambda_{max} = 563$ nm) in the excitation spectra of **5** and **6** reveal that only 21% (**5**) and 83% (**6**) of the excitation energy absorbed by RhB fragments is transferred to PtTBP. At the same time, RhB fluorescence ($\lambda_{max} = 587$ nm) in **5** and **6** is negligible compared to the fluorescence of reference compound **3a**, taken at the same molar concentration (Figure 2B). Therefore, approximately 79% (**5**) and 17% (**6**) of the absorbed energy is consumed in some other process, which in this case is probably ET involving the RhB excited singlet state. This ET will be referred to as ET$_{RhB(S)}$.

The proposed energy-/electron-transfer pathways in RhB–PtTBP systems are shown in Scheme 2. The pathway preferred for our application is shown in the box, and the charge-separated state (CS), formed as a result of the electron transfer, is designated as [RhB–PtTBP]$_{CS}$. Processes ET$_{RhB(S)}$, ET$_{PtTBP(S)}$, and ET$_{PtTBP(T)}$ compete with the preferred pathway by interfering

Two-Photon Oxygen Sensor

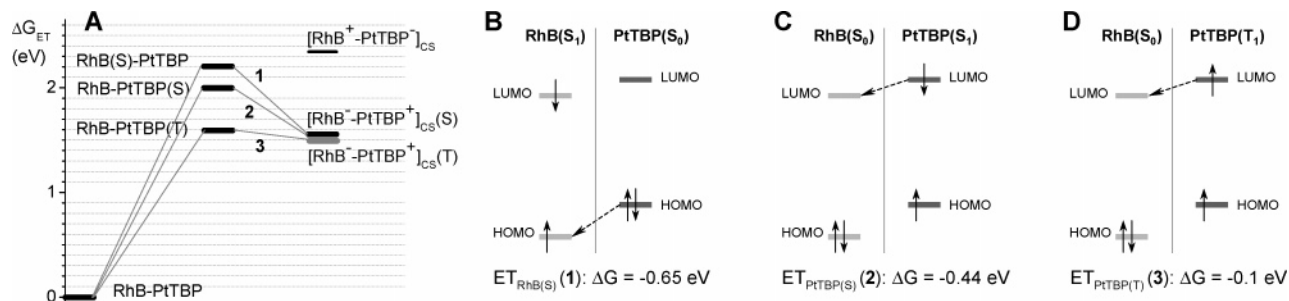*J. Phys. Chem. A, Vol. 111, No. 30, 2007* **6981**

Figure 3. Energy diagram of electron-transfer pathways in photoexcited RhB−PtTBP adducts (A) and frontier orbital levels corresponding to ET$_{RhB(S)}$ (B), ET$_{PtTBP(S)}$ (C), and ET$_{PtTBP(T)}$ (D).

respectively with the FRET, with the intersystem crossing, and with the phosphorescence emission, all leading to the same state [RhB−PtTBP]$_{CS}$. The pathways of annihilation of [RhB−PtTBP]$_{CS}$ remained unidentified and are not shown.

Unfortunately, our attempts to obtain a spectroscopic signature of the charge-separated state [RhB−PtTBP]$_{CS}$ turned out to be unsuccessful (see Supporting Information for details). The transient spectrum of **5** in the window 400−650 nm (set by the limits of the instrument) was entirely dominated by the broad T$_1$ → T$_2$ band of PtTBP (λ_{max} = 463 nm). Similar bands were reported previously for Pd tetraaryltetrabenzoporphyrins.[43c] It is possible that the absorption of the CS state was too weak to be seen on the background of this strong band. Photoinduced electron transfer between RhB and PtTBP nevertheless appears to be the most likely pathway competing with emission in the studied dyads.

B. Electron Transfer. The directionality of the photoinduced ET in RhB−PtTBP adducts could be resolved by substituting spectroscopic and electrochemical data into the Rehm−Weller equation:[54]

$$\Delta G_{ET} = E_{ox}(D) - E_{red}(A) - \Delta E_{00} + w \qquad (1)$$

where ΔG_{ET} is the driving force, $E_{ox}(D)$ is the oxidation potential of the donor, $E_{red}(A)$ is the reduction potential of the acceptor, ΔE_{00} is the excitation energy of the photoexcited component (donor or acceptor), and $w = w_P - w_R$ is the work term, consisting of the Coulombic energies of reactants (w_R) and products (w_P).

The values for **1a** are $E^1_{ox} = +0.75$ V and $E^1_{red} = -1.3$ V vs SCE. In the case of **3a**, a reversible reduction wave was observed at $E_{red} = -0.8$ V, while the oxidation was irreversible and occurred at approximately $E_{ox} = 1.1$ V. These data are consistent with the earlier reported values for Rhodamine B in EtOH solutions.[55] The excitation energy for RhB was estimated from the intersection of its normalized absorption and fluorescence spectra ($\lambda = 565$ nm, $\Delta E_{00} = 2.2$ eV). The value for the PtTBP $\pi-\pi^*$ triplet was derived from the phosphorescence maximum ($\lambda_{max} = 772$ nm, $\Delta E_{00}(T) = 1.61$ eV). The energy of the PtTBP singlet state could be derived from the phosphorescence maximum and the magnitude of the singlet−triplet splitting ($2J = 0.38$ eV), determined from the difference between the S$_0$ → S$_1$ ($\lambda_{max} = 611$ nm) and S$_0$ → T$_1$ ($\lambda_{max} = 762$ nm; see below) absorption maxima: $\Delta E_{00}(S) = 1.99$ eV.

The energy diagram of the ET in RhB−PtTBP systems and the corresponding frontier orbital levels are shown in Figure 3.

The ET from RhB onto PtTBP appears to be endergonic ($\Delta G_{ET} > 0$), in spite of the small favorable Coulombic work term ($w = -0.06$ eV),[56] which is due to the stabilizing interaction between PtTBP anion and RhB dication. (RhB is a cation by itself, and upon the ET onto PtTBP its net charge becomes +2).

The ET in the opposite direction, from PtTBP onto RhB, is exergonic ($\Delta G_{ET} < 0$) for all the excited states, and the work terms in all three cases are close to zero. As discussed above, ET$_{RhB(S)}$ (**1**; $\Delta G_{ET} = -0.65$ eV) competes effectively with the FRET. Assuming the theoretical rate of the FRET as calculated above ($k_{FRET} = 2.5 \times 10^{12}$ s^{-1}) and considering that ratios between efficiencies of ET$_{RhB(S)}$ and FRET in dyads **5** and **6** are 3.76 and 0.20, respectively ($\phi_{ET1}(5)/\phi_{FRET}(5) = 79/21 \approx 3.76$ and $\phi_{ET1}(6)/\phi_{FRET}(6) = 17/83 \approx 0.20$), we arrive at the upper bound estimate for the rate of ET$_{RhB(S)}$, i.e., $k_{RhB(S)} = 10^{12}-10^{13}$ s^{-1}.

Following the FRET, another ET (**2**; ET$_{PtTBP(S)}$), leading to the same charge-separated state is initiated, with the driving force of about 0.2 eV less than that of ET$_{RhB(S)}$. This ET competes directly with the intersystem crossing within the PtTBP macrocycle. The existing photophysical data on Pt porphyrins[20a,c,57] indicate that intersystem crossing occurs in these molecules on a subpicosecond time scale. Therefore, RhB−PtTBP(T) is most certainly generated at a rate comparable to that of ET$_{PtTBP(S)}$.

Once formed, the state RhB−PtTBP(T) in turn undergoes the electron-transfer reaction ET$_{PtTBP(T)}$ (**3**). Since electron-transfer processes generally occur with conservation of spin,[58] the processes ET$_{PtTBP(S)}$ and ET$_{RhB(S)}$ lead to the same singlet biradical charge-separated state, designated in Figure 3A as [RhB$^-$−PtTBP$^+$]$_{CS}$(S). On the contrary, ET$_{PtTBP(T)}$, originating in the triplet state, gives the triplet pair of doublets [RhB$^-$−PtTBP$^+$]$_{CS}$(T). The exchange energy ($2J$) for these transient species is not known, but in general $2J$ values are much smaller for CS states than for individual chromophores.[58] For the purposes of our analysis we assumed that $2J$ was 1/10 of that for PtTBP, i.e., about 0.04 eV. This assumption results in the upper bound estimate for the driving force for ET$_{PtTBP(T)}$, i.e., $\Delta G_{ET} \approx -0.1$ eV.

A straightforward way to prevent unwanted quenching in antenna−triplet emitter complexes would be to reduce the driving force of the ET. It follows from Figure 3A and the Rehm−Weller formula that ΔG_{ET} can be made less negative by either decreasing the reduction potential of the acceptor (RhB) or by increasing the oxidation potential of the donor (PtTBP). At the same time, the HOMO−LUMO gaps of the donor and the acceptor should be kept close in order to maintain large spectral overlap integrals for maximally efficient FRET. Such redox tuning can in principle be accomplished changing the dye's peripheral substitution, i.e., using acceptor groups to increase E_{ox} and donor groups to decrease E_{red}.[35d] σ-Donors and σ-acceptors would be preferred, as those are less likely to alter the spectroscopic properties. Nevertheless, it follows from the orbital diagrams (Figure 3B−D) that by raising the RhB's HOMO too high or lowering the PtTBP's HOMO too low the ET's direction can be reversed. In practice, precise adjustment
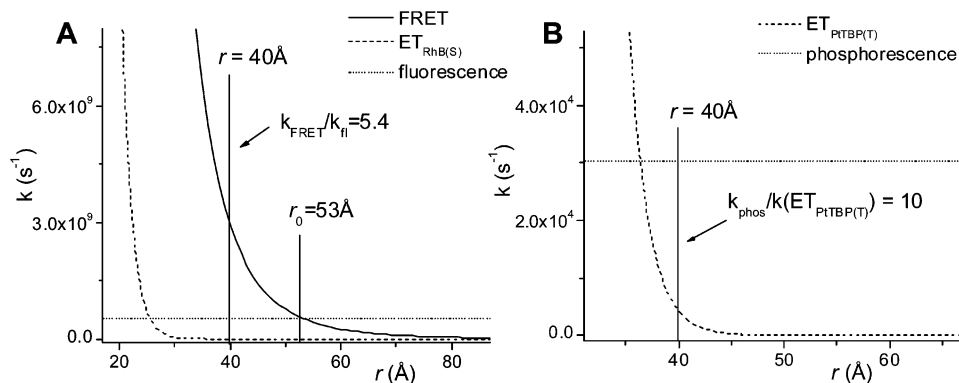
Figure 4. Calculated distance dependences of FRET, $ET_{RhB(S)}$ (A) and $ET_{PtTBP(T)}$ (B), in RhB–PtTBP systems.

of the potentials in order to eliminate the ET might become an extremely tedious task, given that the antenna and the emitter dyes already must satisfy a number of criteria, e.g., high 2PA cross section and strong phosphorescence. Therefore, having an additional mechanism for tuning the ET rates and thus maximizing the sensor performance would be highly desirable.

C. Distance Dependences. Electron-transfer theories predict that rates of intramolecular ET reactions decay exponentially with the distance r between the donor and acceptor sites: $k_{ET} = \nu \exp(-\beta r)$, where parameter β is related to the magnitude of the electronic interaction between the donor and the acceptor and, therefore, is dependent on the nature of the linker between the donor and the acceptor; ν includes the terms dependent on the driving force ΔG_{ET} and the reorganization energy λ.[32,33] Considering that $ET_{RhB(S)}$ and $ET_{PtTBP(S)}$ in our scheme compete with very fast processes, i.e., FRET and intersystem crossing, reducing the efficiencies of these two ET reactions should be relatively easy. Indeed, increasing the separation between PtTBP and RhB by only three σ-bonds (**6** vs **5**) had a pronounced effect on the ratio of the $ET_{RhB(S)}$ and FRET quantum yields ($\phi_{RhB(S)}/\phi_{FRET}$), changing it by as much as 18.4 times, from 3.76 to 0.20. Using the expression for k_{ET} (above) and assuming that (1) at the separation between transition dipoles $r_{FRET} = 13$ Å (as in **5**) the FRET has its theoretical rate ($k_{FRET} = 2.5 \times 10^{12}$ s^{-1}), (2) the edge-to-edge distance between RhB and PtTBP, corresponding to $r_{FRET} = 13$ Å, is $r_{ET} = 7.5$ Å; and (3) the increase in the separation (Δr) going from **5** to **6** equals about 3.4 Å,[59] we obtain $\beta = 5.4 \times 10^7$ cm^{-1} and $\nu = 5.7 \times 10^{14}$ s^{-1}. This value of ν appears to be unrealistically high, as typical pre-exponential factors ν in the distance-dependence equation do not exceed 10^{13} s^{-1}.[33] The error in our calculation is most likely caused by the overestimation of k_{FRET} for dyads **5** and **6**, in which the distances between chromophores are quite short (10–15 Å). As pointed out in a recent study,[60] incomplete orientational averaging ($\kappa^2 < 2/3$) often occurs in molecules connected by short saturated linkers, such as in our models **6** and especially **5**. In addition, at short distances, Förster point-dipole approximation is inaccurate, and the rate of the Coulombic energy transfer must be evaluated by quantum-mechanical methods, which might result in rates lower than those predicted by the Förster model.[60]

Taking this into account, we now assume that the preexponential factor in the case of $ET_{PtTBP(T)}$ is 10^{13} s^{-1},[33] and use parameter β as determined for $ET_{RhB(S)}$. Considering that the rate of the phosphorescence emission of PtTBP **1a** in the absence of oxygen is $k_{phos} = 3.03 \times 10^4$ s^{-1} ($\tau_0 = 33$ μs, Table 1), we estimate that in order for the phosphorescence to be, e.g., 10 times more effective than quenching by the electron transfer ($k_{phos}/k_{PtTBP(T)} = 10$), the chromophores must be placed at a

distance $r_{phos} \approx 40$ Å. At this separation, FRET between RhB and PtTBP should have the rate of 2.9×10^9 s^{-1} and should be about 5.4 times more efficient than RhB fluorescence ($k_{fl} = 1/\tau_{fl} = 5.4 \times 10^8$ s^{-1}). As a result, by separating the chromophores using nonconducting linkers as in **5** or **6** we should be able to gain significantly in the phosphorescence quantum yield while maintaining high efficiency of the FRET. The graphs illustrating these conclusions are shown in Figure 4 and the details of calculations are given in the Supporting Information. It also should be mentioned that at the separation $r_{phos} = 40$ Å the rate of electron transfer $ET_{PtTBP(S)}$ will constitute only a negligible fraction ($\sim 10^{-6}$–10^{-7}) of the intersystem crossing rate within PtTBP molecule.

We would like to emphasize that the assumptions underlying our analysis are quite crude. First, as we already mentioned, Förster's theory might be inaccurate in predicting the energy-transfer rates for compounds with short spacers, as in **5** and **6**. Second, considering the flexibility of the linkers and short distances, direct contacts in **5** and **6** might greatly facilitate ET processes and exceedingly high values for the parameter β, resulting in errors when extrapolating to longer distances. Finally, when calculating the distance at which the phosphorescence can effectively compete with $ET_{PtTBP(T)}$, we assumed that $\nu = 10^{13}$ s^{-1} but used $\beta = 5.4 \times 10^7$ cm^{-1} obtained for $ET_{RhB(S)}$. Therefore, the above discussion provides only a rough estimation of rates and distances; however, it demonstrates the principles of optimization of 2PA antenna–core systems via distance tuning.

RhB–PtTBP Adducts with Polyproline Spacers. It is well-established that saturated spacers can act as "insulators" between donor and acceptor motifs, providing control over electron-transfer rates. The efficiency of this approach has been proven in a variety of models.[33a] Chromophores used in the past to study the distance dependence of electron transfer include heme proteins with porphyrins containing Zn, Mg, Cd, Pt, and Pd and possessing long-lived triplet states[61] as well as other triplet emitters.[33a]

To implement distance tuning in RhB–PtTBP dyads, we considered rigid oligoproline spacers. Oligoprolines (Pro$_n$) are known to form rigid spiral rods in solution[62] and have been employed previously as "spectroscopic rulers".[60,62d,h] The peptide bond in oligoprolines can adopt either cis or trans conformation, with the helix translation step of 3.12 Å (per proline unit) in fully trans conformation vs 1.85 Å in fully cis conformation.[62g] Optical rotatory dispersion (ORD), circular dichroism (CD), and NMR studies of oligoprolines Pro$_n$ suggest that, for $n > 5$, the helix exists exclusively in trans conformation in most solvents (water, alcohol, acetic acid, DMSO, chloroform).[62] For shorter oligoprolines ($n = 2-4$), the cis conformation is also present,
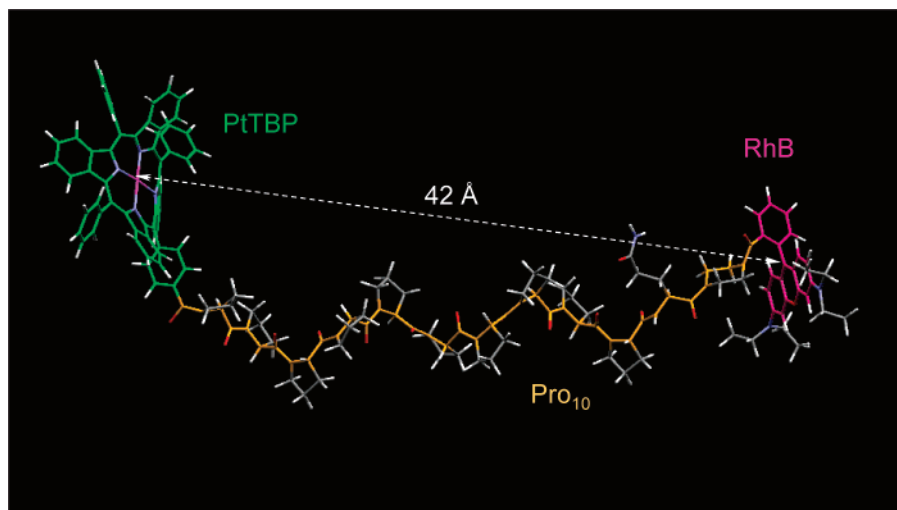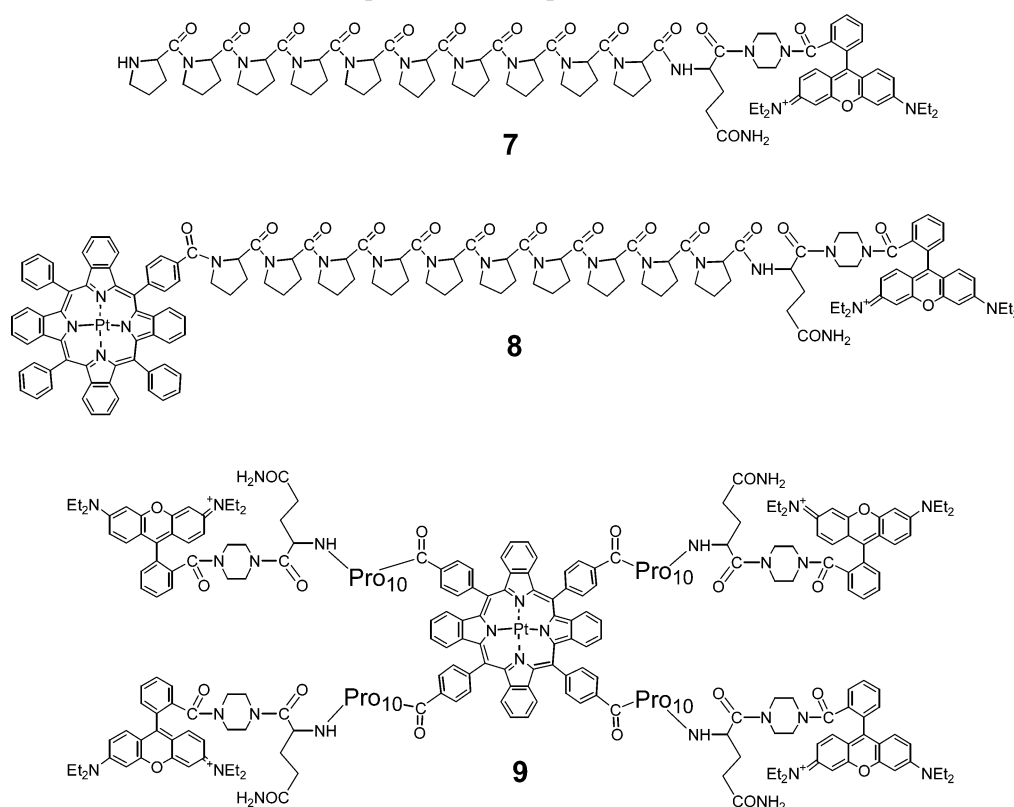
Two-Photon Oxygen Sensor

J. Phys. Chem. A, Vol. 111, No. 30, 2007 **6983**

Figure 5. Optimized structure of RhB−Pro$_{10}$−PtTBP (MM+ force field). Decaproline spacer in its trans conformation provides separation of 42 Å between RhB and PtTBP chromophores.

SCHEME 3: PtTBP−RhB Adducts with Decaproline (Pro$_{10}$) Spacers

especially in less-polar solvents, although trans conformation is still predominant.

Based on the analysis presented above, we chose to connect RhB and PtTBP by decaproline spacers (Pro$_{10}$). In its fully trans conformation, Pro$_{10}$ is approximately 31 Å long, and according to molecular modeling it should provide separation between RhB and PtTBP of about 42 Å (Figure 5). This distance should be adequate for suppressing ET$_{PtTBP(T)}$.

RhB−Pro$_{10}$ conjugate **7** and dyads **8** and **9** are shown in Scheme 3, and their synthesis and characterization are described in detail in the Supporting Information.

Spectroscopy. The emission, excitation, and absorption spectra of compound **8**, as well as of the reference compounds **1a** and **3a**, are shown in Figure 6. As expected, the absorption spectrum of **8** matches that of **5** and presents nearly a superposition of

the spectra of the individual chromophores RhB (**3a**) and PtTBP (**1a**) (Figure 2).

The efficiency of the FRET (ϕ_{FRET} = 0.84) and the phosphorescence quantum yield (ϕ_p = 0.052) of adduct **8** were greatly improved compared to those of **5**. Upon excitation at 520 nm, where the absorbance of PtTBP itself is weak, phosphorescence from adduct **8** was more than 100 times stronger than that of **5** and 10 times stronger than that of the reference porphyrin **1a**. However, the phosphorescence quantum yield of PtTBP in **8** appeared to be only 63% of that for **1a** (0.052 vs 0.083 in EtOH, Table 1). According to our calculations, at the distance of 40 Å the rate of quenching by ET$_{PtTBP(T)}$ should constitute only about 10% of the rate of PtTBP phosphorescence, and the quantum yield of the phosphorescence should be about 0.075. As mentioned earlier, parameter β, used
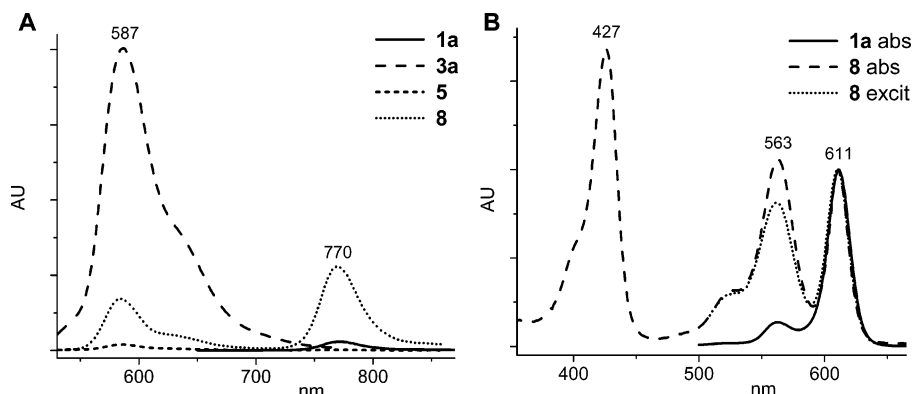
Figure 6. Emission (A), excitation (B), and absorption (B) spectra of adduct **8** and spectra of reference compounds **1a**, **3a**, and **5** in EtOH. All measurements were performed in deoxygenated solutions. (A) The emission spectra were normalized by the absorbance at $\lambda_{ex} = 520$ nm. (B) Excitation spectra were recorded for $\lambda_{em} = 770$ nm. Absorption and excitation spectra were normalized by the intensity at 611 nm (lowest energy S_1 state), which gives rise to the emitting T_1 state.
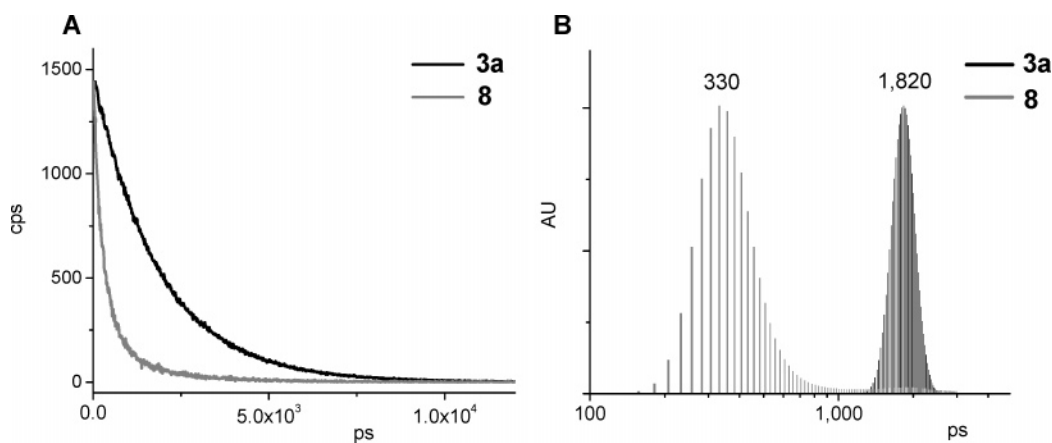

Figure 7. Fluorescence decays of adduct **8** and reference RhB **3a** in MeOH/THF = 1:1, $\lambda_{ex} = 532$ nm (A), and corresponding lifetime distributions (B), obtained by the MEM.

in our calculations, was most likely too high to be applied to $ET_{PtTBP(T)}$, and it is possible that the residual electron transfer was responsible for the decrease in the quantum yield. On the other hand, the phosphorescence quantum yield of **8** practically did not change upon changing the solvent (Table 1), whereas ET rates are typically very sensitive to the solvent dielectric constant. It is therefore also possible that lower phosphorescence quantum yield is an intrinsic property of PtTBP chromophore in **8**.

Emission spectra of **8** and **3a** (Figure 6A) reveal that 84% of RhB fluorescence in **8** is quenched. On the other hand, comparison of the excitation and the absorption spectra of **8** (Figure 6B) shows that the same 84% of the excitation energy is being transferred to PtTBP. Thus, $ET_{RhB(S)}$ and $ET_{PtTBP(S)}$, involving short-lived singlet states, were entirely suppressed by inserting a decaproline spacer between RhB and PtTBP. At the same time, the FRET efficiency in **8** remained quite high ($\phi_{FRET} = 0.84$). Amazingly, calculations based on the Förster theory predict that for the RhB−PtTBP pair the FRET efficiency at the distance of 40 Å should be $\phi_{FRET} = 0.84$! Although such an agreement is probably a coincidence, good correspondence of experimental rates to the Förster model is expected at larger separations between donor and acceptor sites.

The steady-state evaluation of the FRET efficiency was confirmed by fluorescence time resolved measurements. Fluorescence decays of compounds **8** and **3a** and the corresponding lifetime distributions[63] are shown in Figure 7.

In the absence of quenching, **3a** reveals practically a single-exponential decay, i.e., a narrow uniform distribution of lifetimes

(Figure 7B), centered at around $\tau_{av} = 1.82$ ns.[64] In the case of **8**, the distribution moves to shorter lifetimes ($\tau_{av} = 0.33$ ns) and broadens asymmetrically, which is expected for the FRET.[65] The ensemble broadening reflects the distribution of distances between the donor and the acceptor in the dyad. A small second maximum around 1.8 ns is due to the contamination of **8** by unbound RhB. The ratio of the distribution averages for **8** and **3a** corresponds to the FRET efficiency of 0.82, which is very close to the value calculated from the steady-state measurements (0.84).

Our last model compound, **9**, was designed to evaluate how the increase in the number of the antenna chromophores would influence the overall performance of the 2PA phosphorescent sensors. The phosphorescence quantum yield of **9** was 0.028, which again can be explained by the residual quenching via $ET_{PtTBP(T)}$ and taking into account that the number of quenching chromophores (RhB) in **9** is 4 times that in **8**. RhB fluorescence in **9** was quenched by 84%, and the fluorescence lifetime measurements were in good agreement with the spectroscopic data. However, only 55% of the absorbed energy, according to the absorption/excitation spectra, was transferred to the PtTBP. Because distances between the RhB and PtTBP moieties in **9** are the same as in **1**, and $ET_{RhB(S)}$ in **8** was shown to be negligible, quenching of RhB fluorescence by intramolecular electron transfer was ruled out. It is possible that a part of the quenching arises from the formation of nonemitting RhB aggregates within the molecule of **9**. Although Pro_{10} rods are rigid, their linkages to PtTBP *meso*-aryl rings are quite flexible, and RhB termini in **9** can easily experience close contacts with

Two-Photon Oxygen Sensor

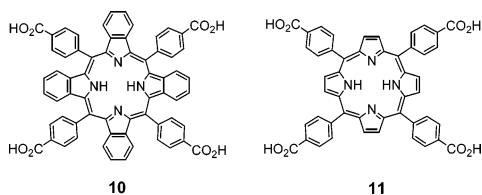*J. Phys. Chem. A, Vol. 111, No. 30, 2007* **6985**

Figure 8. Fluorescent free-base porphyrins used to evaluate 2PA cross sections of Pt tetraaryltetrabenzoporphyrins **1** and **2**.

each other in solution. Self-quenching in rhodamine aggregates is a well-documented phenomenon.[66]

Two-Photon-Excitation Experiments. Two-photon-excitation experiments were designed to (1) estimate 2PA cross sections of core PtTBPs and (2) quantify enhancement of the 2PA-induced phosphorescence via energy transfer from the antenna rhodamines. 2PA cross sections (σ_2) were measured by the relative emission method. To quantify enhancement of the signal in antenna−emitter systems, we used the apparent gain parameter γ,[26] which relates emission from the molecular device D (I^D) to that of the "naked" core C (I^C):

$$\gamma = I^D/I^C \quad (2)$$

In addition, parameter γ_e was used to characterize the expected gain:[67]

$$\gamma_e = \frac{(\sigma_2^A \phi_{FRET}^D + \sigma_2^C)\phi_p^D}{\sigma_2^C \phi_p^C} \quad (3)$$

where σ_2^A and σ_2^C are the 2PA cross sections of the antenna and the core, respectively, the quantum yields of the phosphorescence (ϕ_p) and the FRET (ϕ_{FRET}) are determined from independent linear measurements, and superscripts "A", "C", and "D" refer to the antenna, the core, and the whole device, respectively. Formula 3 is useful because it allows estimation of the 2PA cross section of the device, provided that the FRET and the phosphorescence are independent of the excitation type (1P vs 2P).

As mentioned in the Introduction, in all 2PA antenna/core systems described so far,[26,27] experimental gain coefficients γ were significantly lower than the theoretically expected (γ_e), especially in the systems designed for singlet oxygen sensitization.[27] In these molecules, powerful 2PA antenna dyes (hundreds to thousands of GM units) have been utilized, and the apparent fluorescence quantum yields were high. Nevertheless, gain factors appeared to be tens-to-hundreds of times lower than expected form 2PA cross sections of the antenna.

A. Core Porphyrins. Evaluation of 2PA cross sections of phosphorescent PtTBPs was necessary for quantification of the enhancement effect. Tetraaryltetrabenzoporphyrins possess highly nonplanar molecular structures. Saddling of the porphyrin macrocycle leads to the loss of the center of symmetry and, as a result, should affect its 2PA cross section. In addition, π-extension of the porphyrin macrocycle might have its own influence on the 2PA.

To estimate 2PA cross sections of tetraaryltetrabenzoporphyrins, we used fluorescent nonplanar free-base tetraphenyltetrabenzoporphyrin **10**,[46b] instead of phosphorescent Pt complexes **1** and **2**, and tetracarboxyphenylporphyrin **11**[68] as a reference planar porphyrin (Figure 8).

Measurement by the relative emission method is based on the comparison between emissions from the sample of interest and a standard with the known 2PA cross section. It is necessary that measurements are performed significantly below the

saturation limit, where power dependence of the signal follows the quadratic law. In the case of phosphorescent samples, signal saturation upon excitation by high repetition rate lasers occurs already at quite low powers due to long triplet-state lifetimes (tens of microseconds), whereas measurements at lower powers are inaccurate because of low signal-to-noise ratios. (An indication of the saturation effect has been observed in our experiments.) In addition, triplet states of porphyrins can also be capable of multiphoton absorption, and transitions like $T_1 \rightarrow T_2$ via 2PA can additionally distort measurements of the ground-state 2PA cross sections. Using low repetition rate (e.g., 1 kHz) regenerative amplifiers would help solving these problems, although high per-pulse powers would be required to obtain adequate signals. On the other hand, standard high repetition rate Ti:sapphire oscillators are entirely suitable for measuring fluorescent chromophores with lifetimes below, e.g., 5 ns. Therefore, using fluorescent porphyrin **10** instead of **2** was a convenient way to evaluate the 2PA cross section of the tetraaryltetrabenzoporphyrin macrocycle.

Although porphyrins **10** and **11** are reasonably well soluble in aqueous solutions at basic pH, to avoid aggregation they were bound to bovine serum albumin (BSA, 1% aqueous solution). BSA is known to form complexes with porphyrins and has been used as a porphyrin carrier for construction of oxygen-sensitive probes.[16] Our laser system (76 MHz repetition rate) was tuned to 840 nm. The emission spectra of **10** and **11**, normalized by molar concentrations and extinctions at λ_{ex}, and their power dependence plots are shown in Figure 9. The plot of fluorescence of Rhodamine B, used as a standard, is also shown for comparison.

Power dependences for Rhodamine B and **11** exhibit almost pure second order. In the case of **10** linear absorption was still significant, indicating that for 2P-imaging experiments the wavelength should be shifted further to the red. The values of 2PA cross sections for **10** and **11** were calculated as averages for all excitation powers, in the case of **10** after subtraction of the linear component. The calculations were based on the following data: for **10**, ϵ(646 nm) = 31 000 M^{-1} cm^{-1}, ϕ_{fl} = 0.032;[69] for **11**, ϵ(517 nm) = 19 000 M^{-1} cm^{-1},[70] ϕ_{fl} = 0.15;[69] for Rhodamine B, ϵ(547 nm) = 107 000 M^{-1} cm^{-1},[71] ϕ_{fl} = 0.85,[40] σ_2(840 nm) = 200 GM.[8a] The 2PA cross section of planar porphyrin **11** was found to be low (about 2 GM), consistent with its high symmetry and with earlier reported measurements.[21,26] The 2PA cross section of tetrabenzoporphyrin **10** appeared to be more than 10 times higher than that of **11**, supporting expectations regarding the effects of nonplanarity and, possibly, of π-extension. The σ_2 value of 28 GM for porphyrin **10** is consistent with the earlier reported numbers,[21b] and gives a rough approximation for the 2PA cross sections of PtTBPs **1** and **2**.

Attempts to directly measure 2PA cross sections of PtTBPs led us to an interesting and relevant observation. To monitor phosphorescence of porphyrins **1a** and **2b** and dyads **8** and **9**, we used a time-resolved-phosphorescence measurement system, which was coupled to a regenerative amplifier (30 fs, 1 kHz) operating at λ_{max} = 820 nm. Using the low repetition rate laser allowed collection of complete phosphorescence decays, making it possible to avoid the saturation effects and triplet−triplet excitation via 2PA.

The power dependence plots for both cores **1a** and **2b** turned out to be practically linear (Figure 10A) in spite of the fact that the laser excitation was more than 200 nm away from the lowest energy linear absorption band (λ_{max} = 611−615 nm). Detailed
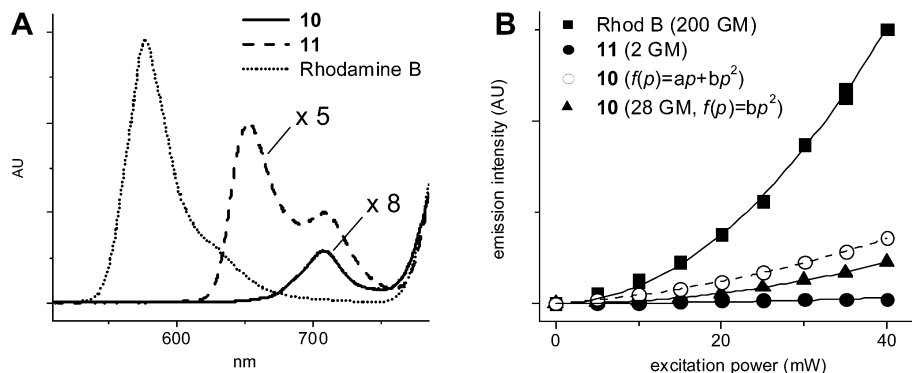
Figure 9. Fluorescence spectra of **10**, **11**, and reference Rhodamine B (A) upon excitation at 840 nm (110 fs). Spectra are normalized by molar concentrations. **10** and **11** were dissolved in 10 mM phosphate buffer in the presence of 1% BSA, pH ~8.5. Rhodamine B was dissolved in EtOH. To obtain power dependences (B), integral intensities of fluorescence were normalized by molar concentrations and fluorescence quantum yields. For **10** (○), the plot was fit to a second-order polymonial, and the linear component was subtracted to render the pure quadratic dependence (▲).
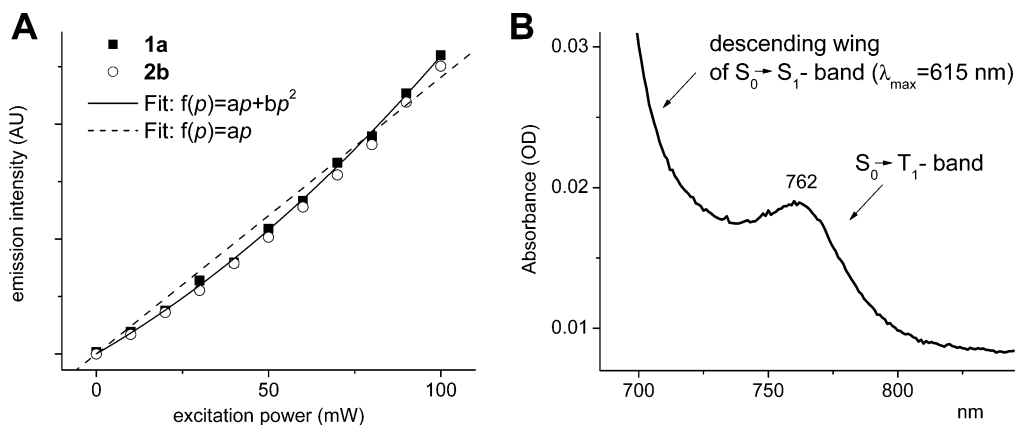

Figure 10. (A) Power dependence plots of the phosphorescence of **1a** and **2b** in deoxygenated DMF upon excitation at 820 nm (30 fs, 1 kHz). (B) $S_0 \rightarrow T_1$ linear absorption band in the spectrum of **2b**: $\lambda_{max} = 762$ nm, $\epsilon = 120$ M^{-1} cm^{-1}.
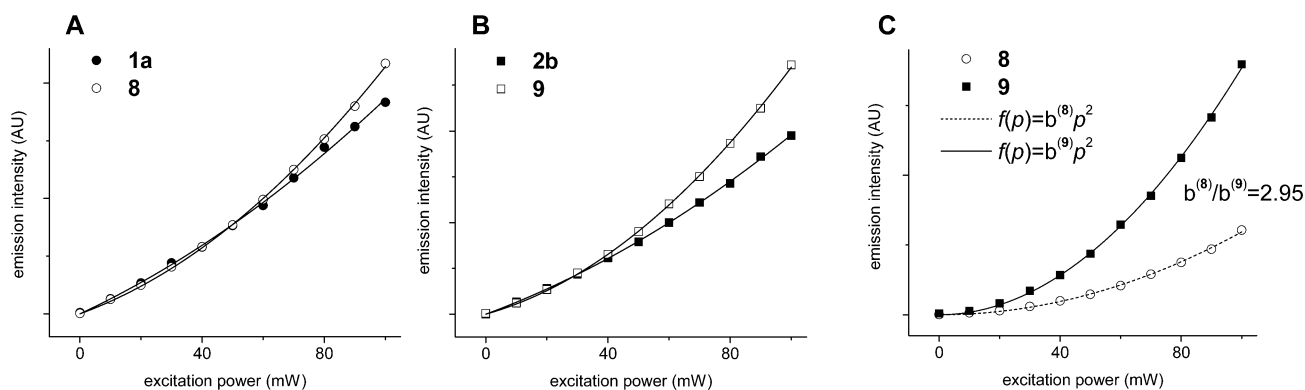

Figure 11. Phosphorescence power dependence plots of adducts **8** and **9** and of reference porphyrins **1a** and **2b** in deoxygenated DMF upon excitation by 30 fs pules ($\lambda_{ex} = 820$ nm, 1 kHz) (A, B). Emission decays were integrated to give the intensity for each excitation power. The plots were normalized by molar concentrations and quantum yields. (C) Quadratic components of the plots for **8** and **9**, obtained by fitting the raw data (A and B) with second-order polynomial and subtracting the obtained linear components. The fits are shown by dashed (**8**) and solid (**9**) lines, yielding the amplification ratio of 2.95.

examination of the absorption spectrum of **2b**, taken at a very high concentration (~10^{-3} M), revealed the presence of a band ($\lambda_{max} = 762$ nm, $\epsilon = 120$ M^{-1} cm^{-1}) which was attributed to $S_0 \rightarrow T_1$ absorption (Figure 10B). The presence of relatively strong spin-forbidden transitions in the spectra of Pd and Pt porphyrins is known from the literature.[57b] These are usually attributed to strong spin−orbit couplings induced by the heavy atoms. However, the extinction coefficient of 120 M^{-1} cm^{-1} is the highest, to our knowledge, reported for direct singlet−triplet absorption. Since the spectrum of the femtosecond source is intrinsically broadened due to the high temporal compression, overlap of the laser with the $S_0 \rightarrow T_1$ band results in the linear

rather than 2P excitation of phosphorescence. From the point of view of 2P imaging this means that using PtTBPs would require laser sources operating above, e.g., 900 nm, where intrinsic 2PA cross sections of PtTBPs may be lower than in the region near 800 nm.

B. RhB−PtTBP Assemblies. The power dependences of the phosphorescence from **8** and **9** are shown in Figure 11A,B together with reference plots for porphyrins **1a** and **2b**. In spite of the interference by the linear $S_0 \rightarrow T_1$ absorption (Figure 10B), the plots for **8** and **9** reveal notable second-order contribution, especially at higher powers, which is evidently due to the 2PA by the RhB antennae. The corresponding plots
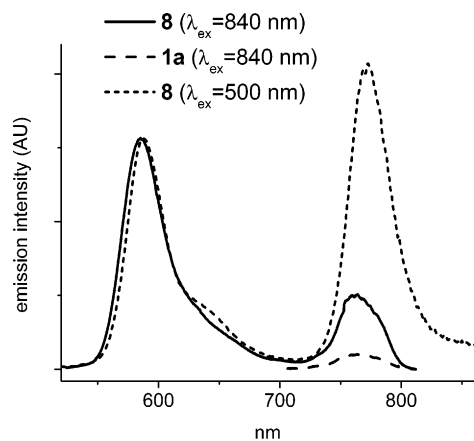
Two-Photon Oxygen Sensor

J. Phys. Chem. A, Vol. 111, No. 30, 2007 **6987**

Figure 12. Emission spectra of adduct **8** and porphyrin **1a** in deoxygenated DMF upon 2P excitation (λ_{ex} = 840 nm, 110 fs, 76 MHz). The spectra were normalized by molar concentrations and corrected to remove the residual excitation leak. The emission spectrum of **8** upon linear excitation (λ_{ex} = 500 nm) (---) was scaled to match the 2PA-induced RhB fluorescence (λ_{max} = 587 nm).

of the reference porphyrins **1a** and **2b** are practically linear. Fitting the normalized data for **8** and **9** by second-order polynomials and subtracting the linear components rendered pure quadratic plots (Figure 11C), from which the enhancement ratio of **9** vs **8** could be calculated as the ratio of coefficients $b^{(9)}/b^{(8)}$ = 2.95. This value is even slightly higher than the theoretically predicted ratio of 2.4, obtained by applying eq 3 to the pair **9** vs **8** and accounting for the difference in the quantum yields of these compounds. To use eq 3, we considered that **9** has three more RhB (σ_2 = 180 GM) units than **8**, and assumed that the 2PA cross section of the core PtTBP in both **8** and **9** is the same as for the model porphyrin **10**, i.e., 28 GM. The corresponding coefficients γ and γ_e (eqs 2 and 3) for **9** vs **8** were in excellent agreement, i.e., 1.25 and 1.28, respectively, indicating linear increase in the 2PA cross section with an increase in the number of RhB antenna units going from mono-RhB to tetra-RhB adduct.

Estimation of the 2PA enhancement effect for compounds **9** and **8** relative to their parent core porphyrins **1a** and **2b** was complicated due to the linear $S_0 \rightarrow T_1$ transition in the absorption spectrum of PtTBP. The apparent enhancement ratios for **8** vs **1a** and **9** vs **2b**, normalized by the phosphorescence quantum yields, were 1.7 and 1.3, respectively, which is substantially lower than the values calculated based on 2PA cross sections of the components, i.e., 6.4 and 15.1. To move the excitation away from $S_0 \rightarrow T_1$ band, we performed measurements of compound **8** and of its reference porphyrin **1a** using the source operating at 840 nm (110 fs, 76 MHz). The corresponding corrected emission spectra are shown in Figure 12.

The long wavelength edges of the phosphorescence peaks of both **8** and **1a** are truncated as a result of the correction for the excitation leak. The laser radiation intensity at above 800 nm was still quite high and diminished the accuracy of the spectral registration. Nevertheless, the apparent gain coefficient γ = 4.2, determined by this method for **8** vs **1a**, was found to be reasonably close to the predicted gain γ_e = 3.7. On the basis of this value of γ, the 2PA cross section of PtTBP in **8** was calculated to be 23.8 GM, which is very close to the value of σ_2 determined for free-base tetrabenzoporphyrin **10**.

The ratios of PtTBP phosphorescence/RhB fluorescence were dramatically different whether 2P or 1P excitation was used. This decrease is likely to be a manifestation of the saturation effect or 2P triplet–triplet absorption in **8**, upon irradiation by

high repetition rate lasers; however, further studies will be required to elucidate the origin of this effect.

Conclusions

Our foregoing experiments demonstrate that enhancement of 2PA-driven triplet-state generation can be accomplished via energy transfer from an appropriately chosen 2PA antenna. However, the molecular architecture of multiphoton phosphorescent systems requires to be manipulated in order to avoid interfering processes, such as intramolecular electron transfer. Several key conclusions, relevant to the design of enhanced phosphorescent sensors and multiphoton singlet oxygen sensitizers, are summarized below.

First, in these systems quenching of excited states, especially long-lived triplet states, by the competing electron transfer is a persistent problem. While triplet electron transfer can be reliably observed and quantified in the case of phosphorescent sensors, quenching of "dark" triplet states in singlet oxygen sensitizers can be not as apparent, and also detrimental to the overall performance. Since most 2PA dyes are conjugated, polarizable molecules, electron transfer is intrinsic to their combination with long-lived photoexcited chromophores. Careful redox tuning of 2PA dyes and/or triplet-state cores should be performed in order to minimize the driving force for unwanted electron-transfer processes.

Second, by using rigid oligoproline spacers for separating RhB antennae from triplet PtTBP cores in RhB−PtTBP assemblies, we have demonstrated that distance tuning can be an effective general method for optimization of 2PA FRET-based triplet systems. A distance can be selected at which electron-transfer processes are suppressed, while long-range Förster energy transfer still occurs with high efficiency.

Third, the presence of "hidden" low-energy transitions in the spectra of triplet-state emitters, e.g., metalloporphyrins with increased π-conjugation, might present a problem for excitation by a pure multiphoton mechanism. Such transitions are intrinsic to the systems with enhanced singlet−triplet conversion pathways, e.g., by the heavy atom effect. For example, in the case of PtTBP, a strong spin-forbidden $S_0 \rightarrow T_1$ transition could be observed in the close vicinity of the Ti:sapphire laser spectrum, preventing efficient excitation by the 2PA mechanism.

Finally, our measurements demonstrate that the loss of the center of symmetry due to nonplanar distortion of the porphyrin macrocycle and its π-extension lead to a significant increase in 2PA cross section. For example, the 2PA cross section of saddled tetraaryltetrabenzoporphyrins in the region of 800 nm was estimated to be about an order of magnitude higher than that of a planar tetraarylporphyrin. The possibility of using asymmetric phosphorescent porphyrins directly as 2PA oxygen sensors will be explored in the future.

It should be mentioned that phosphorescence of all PtTBP-based molecules studied in this work was found to be extremely oxygen sensitive in organic solutions. However, determination of the actual Stern−Volmer oxygen quenching constants for RhB−PtTBP assemblies will need to be accomplished after modifying these systems to solubilize them in aqueous environments, e.g., by attaching appropriate dendritic arms.[26] It is not clear at this point whether RhB−PtTBP systems themselves will become the probes of choice for 2P oxygen microscopy, primarily because of the difficulties associated with hidden S_0-T_1 bands of PtTBP cores. Nevertheless, analysis of these systems appeared to be informative and useful for future construction of optimized 2PA-enhanced functional triplet core systems.

6988 *J. Phys. Chem. A, Vol. 111, No. 30, 2007*

Finikova et al.

Supporting Information Available: Experimental details, synthetic procedures, and characterization data for the compounds described in this paper; complete ref 9b. This material is available free of charge via the Internet at http://pubs.acs.org

References and Notes

(1) The quantity σ_2 is commonly referred to as the "two-photon-absorption cross section," although it is not an area (see, for example: www.drbio.cornell.edu/MPE/mpe.html). It is the proportionality coefficient between the photon absorption rate per molecule (β) and the time-averaged square of the photon flux Φ: $\beta = \sigma_2 \langle \Phi^2 \rangle$. σ_2 is measured in GM (Göppert-Mayer) units: 1 GM $= 10^{-50}$ cm^4 s photon^{-1}.

(2) Denk, W.; Strickler, J. H.; Webb, W. W. *Science* **1990**, *248*, 73–76.

(3) For recent reviews, see: (a) Svoboda, K.; Yasuda, R. *Neuron* **2006**, *50*, 823–839. (b) Rothstein, E. C.; Nauman, M.; Chesnick, S.; Balaban, R. S. *J. Microsc. (Oxford)* **2006**, *222*, 58–64. (c) Helmchen, F.; Denk, W. *Nat. Methods* **2005**, *2*, 932–940. (d) Helmchen, F.; Denk, W. *Curr. Opin. Neurobiol.* **2002**, *12*, 593–601.

(4) Göppert-Mayer, M. *Ann. Phys.* **1931**, *9*, 273.

(5) Parthenopoulos, D. A.; Rentzepis, P. M. *Science* **1989**, *245*, 843–845.

(6) (a) He, G. S.; Bhawalkar, J. D.; Zhao, C. F.; Prasad, P. N. *Appl. Phys. Lett.* **1995**, *67*, 2433–2435. (b) Lin, T. C.; Chung, S. J.; Kim, K. S.; Wang, X. P.; He, G. S.; Swiatkiewicz, J.; Pudavar, H. E.; Prasad, P. N. *Polymers for Photonics Applications II*; Advances in Polymer Science 161; Springer: Berlin, 2003; pp 157–193.

(7) (a) Bhawalkar, D. D.; Kumar, N. D.; Zhao, C. F.; Prasad, P. N. *J. Clin. Med. Surg.* **1997**, *37*, 210–204. (b) König, K. *J. Microsc.* **2000**, *200*, 83–104, and references therein.

(8) (a) Xu, C.; Webb, W. W. *J. Opt. Soc. Am. B* **1996**, *13*, 481–491. (b) Albota, M. A.; Xu, C.; Webb, W. W. *Appl. Opt.* **1998**, *37*, 7352–7356.

(9) Examples of 2PA chromophores based on π-conjugated donor–acceptor systems: (a) Mongin, O.; Porres, L.; Charlot, M.; Katan, C.; Blanchard-Desce, M. *Chem.—Eur. J.* **2007**, *13*, 1481–1498. (b) Chung, S. J.; et al. *J. Am. Chem. Soc.* **2006**, *128*, 14444–14445. (c) Morales, A. R.; Belfield, K. D.; Hales, J. M.; Van Stryland, E. W.; Hagan, D. J. *Chem. Mater.* **2006**, *18*, 4972–4980. (d) Krishna, T. R.; Parent, M.; Werts, M. H. V.; Moreaux, L.; Gmouh, S.; Charpak, S.; Caminade, A. M.; Majoral, J. P.; Blanchard-Desce, M. *Angew. Chem., Int. Ed.* **2006**, *45*, 4645–4648. (e) Kato, S.; Matsumoto, T.; Shigeiwa, M.; Gorohmaru, H.; Maeda, S.; Ishi-i, T.; Mataka, S. *Chem.—Eur. J.* **2006**, *12*, 2303–2317. (f) Huang, P. H.; Shen, J. Y.; Pu, S. C.; Wen, Y. S.; Lin, J. T.; Chou, P. T.; Yeh, M. C. P. *J. Mater. Chem.* **2006**, *16*, 850–857. (g) Hayek, A.; Nicoud, J. F.; Bolze, F.; Bourgogne, C.; Baldeck, P. L. *Angew. Chem., Int. Ed.* **2006**, *45*, 6466–6469. (h) Zheng, Q. D.; He, G. S.; Prasad, P. N. *J. Mater. Chem.* **2005**, *15*, 579–587. (i) Chung, S. J.; Rumi, M.; Alain, V.; Barlow, S.; Perry, J. W.; Marder, S. R. *J Am. Chem. Soc.* **2005**, *127*, 10844–10845. (j) Woo, H. Y.; Hong, J. W.; Liu, B.; Mikhailovsky, A.; Korystov, D.; Bazan, G. C. *J. Am. Chem. Soc.* **2005**, *127*, 820–821. (k) Oliveira, S. L.; Correa, D. S.; Misoguti, L.; Constantino, C. J. L.; Aroca, R. F.; Zilio, S. C.; Mendonca, C. R. *Adv. Mater.* **2005**, *17*, 1890.

(10) Examples of 2PA chromophores based on porphyrin conjugates and arrays: (a) Karotki, A.; Drobizhev, M.; Dzenis, Y.; Taylor, P. N.; Anderson, H. L.; Rebane, A. *Phys. Chem. Chem. Phys.* **2004**, *6*, 7–10. (b) Drobizhev, M.; Stepanenko, Y.; Dzenis, Y.; Karotki, A.; Rebane, A.; Taylor, P. N.; Anderson, H. L. *J. Am. Chem. Soc.* **2004**, *126*, 15352–15353. (c) Ogawa, K.; Ohashi, A.; Kobuke, Y.; Kamada, K.; Ohta, K. *J. Phys. Chem. B* **2005**, *109*, 22003–22012. (d) Drobizhev, M.; Stepanenko, Y.; Rebane, A.; Wilson, C. J.; Screen, T. E. O.; Anderson, H. L. *J. Am. Chem. Soc.* **2006**, *128*, 12432–12433. (e) Ahn, T. K.; Kim, K. S.; Kim, D. Y.; Noh, S. B.; Aratani, N.; Ikeda, C.; Osuka, A.; Kim, D. *J. Am. Chem. Soc.* **2006**, *128*, 1700–1704.

(11) Examples of 2PA chromophores based on modified porphyrins: (a) Ahn, T. K.; Kwon, J. H.; Kim, D. Y.; Cho, D. W.; Jeong, D. H.; Kim, S. K.; Suzuki, M.; Shimizu, S.; Osuka, A.; Kim, D. *J. Am. Chem. Soc.* **2005**, *127*, 12856–12861. (b) Kwon, J. H.; Ahn, T. K.; Yoon, M. C.; Kim, D. Y.; Koh, M. K.; Kim, D.; Furuta, H.; Suzuki, M.; Osuka, A. *J. Phys. Chem. B* **2006**, *110*, 11683–11690. (c) Rath, H.; Prabhuraja, V.; Chandrashekar, T. K.; Nag, A.; Goswami, D.; Joshi, B. S. *Org. Lett.* **2006**, *8*, 2325–2328. (d) Kurotobi, K.; Kim, K. S.; Noh, S. B.; Kim, D.; Osuka, A. *Angew. Chem., Int. Ed.* **2006**, *45*, 3944–3947. (e) Kim, D. Y.; Alm, T. K.;

Kwon, J. H.; Kim, D.; Ikeue, T.; Aratani, N.; Osuka, A.; Shigeiwa, M.; Maeda, S. *J. Phys. Chem. A* **2005**, *109*, 2996–2999. (f) Inokuma, Y.; Ono, N.; Uno, H.; Kim, D. Y.; Noh, S. B.; Kim, D.; Osuka, A. *Chem. Commun.* **2005**, 3782–3784.

(12) Examples of 2PA chromophores based on dendrimers: (a) Adronov, A.; Fréchet, J. M. J.; He, G. S.; Kim, K. S.; Chung, S. J.; Swiatkiewicz, J.; Prasad, P. N. *Chem. Mater.* **2000**, *12*, 2838. (b) Drobizhev, M.; Karotki, A.; Rebane, A.; Spangler, C. W. *Opt. Lett.* **2001**, *26*, 1081–1083. (c) Drobizhev, M.; Karotki, A.; Dzenis, Y.; Rebane, A.; Suo, Z. Y.; Spangler, C. W. *J. Phys. Chem. B* **2003**, *107*, 7540–7543. (d) Brousmiche, D. W.; Serin, J. M.; Fréchet, J. M. J.; He, G. S.; Lin, T. C.; Chung, S. J.; Prasad, P. N.; Kannan, R.; Tan, L. S. *J. Phys. Chem. B* **2004**, *108*, 8592–8600. (e) Wei, P.; Bi, X. D.; Wu, Z.; Xu, Z. *Org. Lett.* **2005**, *7*, 3199–3202. (f) Mongin, O.; Krishna, T. R.; Werts, M. H. V.; Caminade, A. M.; Majoral, J. P.; Blanchard-Desce, M. *Chem. Commun.* **2006**, 915–917. (g) Bhaskar, A.; Guda, R.; Haley, M. M.; Goodson, T. *J. Am. Chem. Soc.* **2006**, *128*, 13972–13973.

(13) 2PA porphyrin aggregates: (a) Collini, E.; Ferrante, C.; Bozio, R. *J. Phys. Chem. B* **2005**, *109*, 2–5. (b) Ray, P. C.; Sainudeen, Z. *J. Phys. Chem. A* **2006**, *110*, 12342–12347.

(14) Quantum dots: Larson, D. R.; Zipfel, W. R.; Williams, R. M.; Clark, S. W.; Bruchez, M. P.; Wise, F. W.; Webb, W. W. *Science* **2003**, *300*, 1434–1436.

(15) (a) Albota, M.; Beljonne, D.; Bredas, J. L.; Ehrlich, J. E.; Fu, J. Y.; Heikal, A. A.; Hess, S. E.; Kogej, T.; Levin, M. D.; Marder, S. R.; McCord-Maughon, D.; Perry, J. W.; Rockel, H.; Rumi, M.; Subramaniam, C.; Webb, W. W.; Wu, X. L.; Xu, C. *Science* **1998**, *281*, 1653–1656. (b) Rumi, M.; Ehrlich, J. E.; Heikal, A. A.; Perry, J. W.; Barlow, S.; Hu, Z. Y.; McCord-Maughon, D.; Parker, T. C.; Rockel, H.; Thayumanavan, S.; Marder, S. R.; Beljonne, D.; Bredas, J. L. *J. Am. Chem. Soc.* **2000**, *122*, 9500–9510.

(16) (a) Vanderkooi, J. M.; Maniara, G.; Green, T. J.; Wilson, D. F. *J. Biol. Chem.* **1987**, *262*, 5476–5483. (b) Wilson, D. F.; Vinogradov, S. A. In *Handbook of Biomedical Fluorescence*; Mycek, M.-A., Pogue B. W., Eds.; Marcel Dekker, Inc.: New York, 2003; Chapter 17.

(17) We limit our scope by the literature on oxygen measurements using molecular probes introduced directly into the medium of interest, e.g., blood or interstitial space. In addition, there is a large area of research covering solid-state phosphorescent oxygen sensors. For a review, see: Demas, J. N.; DeGraff, B. A.; Coleman, P. B. *Anal. Chem.* **1999**, *71*, 793A–800A.

(18) For the latest examples, see: (a) Pittman, R. N. *Microcirculation* **2005**, *12*, 59–70. (b) Ferreira, L. F.; McDonough, P.; Behnke, B. J.; Musch, T. I.; Poole, D. C. *Resp. Physiol. Neurobiol.* **2006**, *153*, 237–249. (c) Johannes, T.; Mik, E. G.; Ince, C. *J. Appl. Physiol.* **2006**, *100*, 1301–1310. (d) Tsai, A. G.; Friesenecker, B.; Cabrales, P.; Hangai-Hoger, N.; Intaglietta, M. *Curr. Opin. Nephrol. Hypertens.* **2006**, *15*, 67–71. (e) Wilson, D. F.; Lee, W. M. F.; Makonnen, S.; Finikova, O.; Apreleva, S.; Vinogradov, S. A. *J. Appl. Physiol.* **2006**, *101*, 1648–1656. (f) Zaitseva, T.; Schultz, S.; Schears, G.; Pastuszko, P.; Markowitz, S.; Greeley, W.; Wilson, D. F.; Pastuszko, A. *Ann. Thoracic Surg.* **2006**, *82*, 2247–2253.

(19) For examples, see: (a) Rumsey, W. L.; Vanderkooi, J. M.; Wilson, D. F. *Science* **1988**, *241*, 1649–1652. (b) Plant, R. L.; Burns, D. H. *Appl. Spectrosc.* **1993**, *47*, 1594–1599. (c) Vinogradov, S. A.; Lo, L.-W.; Jenkins, W. T.; Evans, S. M.; Koch, C.; Wilson, D. F. *Biophys. J.* **1996**, *70*, 1609–1617. (d) Smith, L. M.; Golub, A. S.; Pittman, R. N. *Microcirculation* **2002**, *9*, 389–395. (e) Golub, A. S.; Pittman, R. N. *FASEB J.* **2002**, *16*, A520–A520. (f) Shonat, R. D.; Kight, A. C. *Ann. Biomed. Eng.* **2003**, *31*, 1084–1096. (g) Apreleva, S. V.; Wilson, D. F.; Vinogradov, S. A. *Appl. Opt.* **2006**, *45*, 8547–8559. (h) Shahidi, M.; Shakoor, A.; Blair, N. P.; Mori, M.; Shonat, R. D. *Curr. Eye Res.* **2006**, *31*, 357–366.

(20) (a) Eastwood, D.; Gouterman, M. *J. Mol. Spectrosc.* **1970**, *35*, 359–375. (b) Callis, J. B.; Knowles, J. M.; Gouterman, M. *J. Phys. Chem.* **1973**, *77*, 154–156. (c) Kim, D. H.; Holten, D.; Gouterman, M.; Buchler, J. W. *J. Am. Chem. Soc.* **1984**, *106*, 4015–4017. (d) Vinogradov, S. A.; Wilson, D. F. *J. Chem. Soc., Perkin Trans. 2* **1995**, 103–111.

(21) (a) Kruk, M.; Karotki, A.; Drobizhev, M.; Kuzmitsky, V.; Gael, V.; Rebane, A. *J. Lumin.* **2003**, *105*, 45–55. (b) Karotki, A.; Drobizhev, M.; Kruk, M.; Spangler, C.; Nickel, E.; Mamardashvili, N.; Rebane, A. *J. Opt. Soc. Am. B* **2003**, *20*, 321.5. (c) Karotki, A.; Khurana, M.; Lepock, J. R.; Wilson, B. C. *Photochem. Photobiol.* **2006**, *82*, 443–452.

(22) (a) Castellano, F. N.; Malak, H.; Gryczynski, I.; Lakowicz, J. R. *Inorg. Chem.* **1997**, *36*, 5548–5551. (b) Lakowicz, J. R.; Castellano, F. N.; Gryczynski, I.; Gryczynski, Z.; Dattelbaum, J. D. *J. Photochem. Photobiol. Chem.* **1999**, *122*, 95–101.

(23) Although 2P excitation of metalloporphyrins has been reported to induce their phosphorescence (Mik, E. G.; van Leeuwen, T. G.; Raat, N. J.; Ince, C. *J. Appl. Physiol.* **2004**, *97*, 1962–1969), for biological imaging applications 2PA cross sections of phosphorescent probes must be significantly higher.

(24) (a) Karotki, A.; Drobizhev, M.; Kruk, M.; Spangler, C.; Nickel, E.; Mamardashvili, N.; Rebane, A. *J. Opt. Soc. Am. B* **2003**, *20*, 321–332. (b) Drobizhev, M.; Karotki, A.; Kruk, M.; Mamardashvili, N. Z.; Rebane, A. *Chem. Phys. Lett.* **2002**, *361*, 504–512. (c) Drobizhev, M.; Karotki, A.;

Two-Photon Oxygen Sensor

J. Phys. Chem. A, Vol. 111, No. 30, 2007 **6989**

Kruk, M.; Rebane, A. *Chem. Phys. Lett.* **2002**, *355*, 175−182. (d) Drobizhev, M.; Meng, F. Q.; Rebane, A.; Stepanenko, Y.; Nickel, E.; Spangler, C. W. *J. Phys. Chem. B* **2006**, *110*, 9802−9814. (e) Morone, M.; Beverina, L.; Abbotto, A.; Silvestri, F.; Collini, E.; Ferrante, C.; Bozio, R.; Pagani, G. A. *Org. Lett.* **2006**, *8*, 2719−2722.

(25) Duncan, T. V.; Susumu, K.; Sinks, L. E.; Therien, M. J. *J. Am. Chem. Soc.* **2006**, *128*, 9000−9001.

(26) Briñas, R. P.; Troxler, T.; Hochstrasser, R. M.; Vinogradov, S. A. *J. Am. Chem. Soc.* **2005**, *127*, 11851−11862.

(27) (a) Dichtel, W. R.; Serin, J. M.; Edder, C.; Fréchet, J. M. J.; Matuszewski, M.; Tan, L. S.; Ohulchanskyy, T. Y.; Prasad, P. N. *J. Am. Chem. Soc.* **2004**, *126*, 5380−5381. (b) Oar, M. A.; Serin, J. M.; Dichtel, W. R.; Fréchet, J. M. J. *Chem. Mater.* **2005**, *17*, 2267−2275.

(28) A similar idea has recently been utilized to photochemically release nitric oxide upon 2P excitation: Wecksler, S. R.; Mikhailovsky, A.; Korystov, D.; Ford, P. C. *J. Am. Chem. Soc.* **2006**, *128*, 3831−3837.

(29) (a) Vinogradov, S. A.; Lo, L. W.; Wilson, D. F. *Chem.−Eur. J.* **1999**, *5*, 1338−1347. (b) Rozhkov, V.; Wilson, D.; Vinogradov, S. *Macromolecules* **2002**, *35*, 1991−1993. (c) Rietveld, I. B.; Kim, E.; Vinogradov, S. A. *Tetrahedron* **2003**, *59*, 3821−3831.

(30) Förster, T. *Fluorenzenz Organische Verbindungen*; Vandenhoech and Ruprech: Gottingen, 1951.

(31) Turro, N. J. *Modern Molecular Photochemistry*; University Science Books: Sausalito, CA, 1991.

(32) Marcus, R. A.; Sutin, N. *Biochim. Biophys. Acta* **1985**, *811*, 265.

(33) For reviews, see: (a) Isied, S. S.; Ogawa, M. Y.; Wishart, J. F. *Chem. Rev.* **1992**, *92*, 381−394. (b) *Electron Transfer in Chemistry*; Balzani, V., Ed.; Wiley-VCH: Weinheim, 2001.

(34) Moser, C. C.; Page, C. C.; Cogdell, R. J.; Barber, J.; Wraight, C. A.; Dutton, P. L. *Adv. Protein Chem. Membr. Proteins* **2003**, *63*, 71−109.

(35) For books and reviews, see: (a) *Photoinduced Electron Transfer*; Mattay, J., Ed.; Springer-Verlag: New York, 1990. (b) Wasielewski, M. R. *Chem. Rev.* **1992**, *92*, 435−461. (c) Winkler, J. R.; Gray, H. B. *Chem. Rev.* **1992**, *92*, 369−379. (d) Gust, D.; Moore, T. A. In *The Porphyrin Handbook*; Kadish, K. M., Smith, K. M., Guilard, R., Eds.; Academic Press: New York, 2000; Vol. 8, Chapter 57. (e) Balzani, V.; Juris, A. *Coord. Chem. Rev.* **2001**, *211*, 97−115. (f) Nantalaksakul, A.; Reddy, D. R.; Bardeen, C. J.; Thayumanavan, S. *Photosynth. Res.* **2006**, *87*, 133−150.

(36) For recent reports, see: (a) Xiao, S. Q.; El-Khouly, M. E.; Li, Y. L.; Gan, Z. H.; Liu, H. B.; Jiang, L.; Araki, Y.; Ito, O.; Zhu, D. *J. Phys. Chem. B* **2005**, *109*, 3658−3667. (b) Yan, X. Z.; Goodson, T.; Imaoka, T.; Yamamoto, K. *J. Phys. Chem. B* **2005**, *109*, 9321−9329. (c) Ahn, T. S.; Nantalaksakul, A.; Dasari, R. R.; Al-Kaysi, R. O.; Muller, A. M.; Thayumanavan, S.; Bardeen, C. J. *J. Phys. Chem. B* **2006**, *110*, 24331−24339. (d) Cho, S.; Li, W. S.; Yoon, M. C.; Ahn, T. K.; Jiang, D. L.; Kim, J.; Aida, T.; Kim, D. *Chem.−Eur. J.* **2006**, *12*, 7576−7584. (e) Flamigni, L.; Talarico, A. M.; Ventura, B.; Sooambar, C.; Solladie, N. *Eur. J. Inorg. Chem.* **2006**, 2155−2165. (f) Ito, F.; Ishibashi, Y.; Khan, S. R.; Miyasaka, H.; Kameyama, K.; Morisue, M.; Satake, A.; Ogawa, K.; Kobuke, Y. *J. Phys. Chem. A* **2006**, *110*, 12734−12742. (g) Kodis, G.; Terazono, Y.; Liddell, P. A.; Andreasson, J.; Garg, V.; Hambourger, M.; Moore, T. A.; Moore, A. L.; Gust, D. *J. Am. Chem. Soc.* **2006**, *128*, 1818−1827. (h) Pettersson, K.; Kyrychenko, A.; Ronnow, E.; Ljungdahl, T.; Martensson, J.; Albinsson, B. *J. Phys. Chem. A* **2006**, *110*, 310−318. (i) Ermilov, E. A.; Tannert, S.; Werncke, T.; Choi, M. T. M.; Ng, D. K. P.; Röder, B. *Chem. Phys.* **2006**, *328*, 428−437.

(37) (a) Joshi, M. P.; Swiatkiewicz, J.; Xu, F. M.; Prasad, P. N. *Opt. Lett.* **1998**, *23*, 1742−1744. (b) Chung, S. J.; Lin, T. C.; Kim, K. S.; He, G. S.; Swiatkiewicz, J.; Prasad, P. N.; Baker, G. A.; Bright, F. V. *Chem. Mater.* **2001**, *13*, 4071−4076. (c) Chiang, L. Y.; Padmawar, P. A.; Canteenwala, T.; Tan, L. S.; He, G. S.; Kannan, R.; Vaia, R.; Lin, T. C.; Zheng, Q. D.; Prasad, P. N. *Chem. Commun.* **2002**, 1854−1855. (d) Brousmiche, D. W.; Serin, J. M.; Fréchet, J. M. J.; He, G. S.; Lin, T. C.; Chung, S. J.; Prasad, P. N. *J. Am. Chem. Soc.* **2003**, *125*, 1448−1449. (e) He, G. S.; Lin, T. C.; Cui, Y. P.; Prasad, P. N.; Brousmiche, D. W.; Serin, J. M.; Fréchet, J. M. J. *Opt. Lett.* **2003**, *28*, 768−770. (f) Brousmiche, D. W.; Serin, J. M.; Fréchet, J. M. J.; He, G. S.; Lin, T. C.; Chung, S. J.; Prasad, P. N.; Kannan, R.; Tan, L. S. *J. Phys. Chem. B* **2004**, *108*, 8592−8600.

(38) For a theoretical treatment, see: (a) Andrews, D. L.; Bradshaw, D. S. *J. Chem. Phys.* **2004**, *121*, 2445−2454. (b) Bradshaw, D. S.; Andrews, D. L. *Chem. Phys. Lett.* **2006**, *430*, 191−194.

(39) In a recent study (Kauert, M.; Stoller, P. C.; Frenz, M.; Ricka, J. *Opt. Express* **2006**, *14*, 8434−8447) the 2PA cross section of Rhodamine B in MeOH was rigorously measured and shown to have the value $\sigma_2 =$ 24.4 GM at 800 nm, which is about 6 times lower than that reported by Xu and Webb ($\sigma_2 = 150$ GM).[8a] Nevertheless, we chose to use the commonly referred to value from ref 8a in order to facilitate comparison with the current literature.

(40) Several values have been reported in the literature for the fluorescence quantum yield of Rhodamine B, ranging from 0.41 to 0.97 (Demas, J. N.; Crosby, G. A. *J. Phys. Chem.* **1971**, *75*, 991−1024). We

used the value of 0.5, reported by Karstens and Kobs[41] and rigorously confirmed by our own measurements.

(41) Karstens, T.; Kobs, K. *J. Phys. Chem.* **1980**, *84*, 1871−1872.

(42) Nguyen, T.; Francis, M. B. *Org. Lett.* **2003**, *5*, 3245−3248.

(43) (a) Tsvirko, M. P.; Sapunov, V. V.; Soloviyev, K. N. *Opt. Spektrosk. (Russ.)* **1973**, *34*, 1094−1100. (b) Aartsma, T. J.; Gouterman, M.; Jochum, C.; Kwiram, A. L.; Pepich, B. V.; Williams, L. D. *J. Am. Chem. Soc.* **1982**, *104*, 6278−6283. (c) Rogers, J. E.; Nguyen, K. A.; Hufnagle, D. C.; McLean, D. G.; Su, W. J.; Gossett, K. M.; Burke, A. R.; Vinogradov, S. A.; Pachter, R.; Fleitz, P. A. *J. Phys. Chem. A* **2003**, *107*, 11331−11339. (d) Finikova, O. S.; Cheprakov, A. V.; Vinogradov, S. A. *J. Org. Chem.* **2005**, *70*, 9562−9572.

(44) (a) Finikova, O.; Cheprakov, A.; Beletskaya, I.; Vinogradov, S. *Chem. Commun.* **2001**, 261−262. (b) Finikova, O. S.; Cheprakov, A. V.; Beletskaya, I. P.; Carroll, P. J.; Vinogradov, S. A. *J. Org. Chem.* **2004**, *69*, 522−535.

(45) For calculations of the Förster distance r_0, energy-transfer rates, and electron-transfer rates, see the Supporting Information.

(46) (a) Cheng, R. J.; Chen, Y. R.; Wang, S. L.; Cheng, C. Y. *Polyhedron* **1993**, *12*, 1353−1360. (b) Finikova, O. S.; Cheprakov, A. V.; Carroll, P. J.; Dalosto, S.; Vinogradov, S. A. *Inorg. Chem.* **2002**, *41*, 6944−6946.

(47) For examples, see: (a) Charlesworth, P.; Truscott, T. G.; Kessel, D.; Medforth, C. J.; Smith, K. M. *J. Chem. Soc., Faraday Trans.* **1994**, *90*, 1073−1076. (b) Gentemann, S.; Medforth, C. J.; Forsyth, T. P.; Nurco, D. J.; Smith, K. M.; Fajer, J.; Holten, D. *J. Am. Chem. Soc.* **1994**, *116*, 7363. (c) Gentemann, S.; Medforth, C. J.; Ema, T.; Nelson, N. Y.; Smith, K. M.; Fajer, J.; Holten, D. *Chem. Phys. Lett.* **1995**, *245*, 441−447. (d) Sazanovich, I. V.; Galievsky, V. A.; van Hoek, A.; Schaafsma, T. J.; Malinovskii, V. L.; Holten, D.; Chirvony, V. S. *J. Phys. Chem. B* **2001**, *105*, 7818.

(48) Seybold, P. G.; Gouterman, M. *J. Mol. Spectrosc.* **1969**, *31*, 1.

(49) If measured against Rhodamine B in methanol ($\phi_{fl} = 0.5$),[40] H$_2$-TPP in deoxygenated benzene exhibits the absolute fluorescence quantum yield $\phi_{fl} = 0.048$. A much higher value for H$_2$TPP ($\phi_{fl} = 0.11$) was reported by Seybold and Gouterman[48] and became a standard reference in porphyrin spectroscopy. The yield of $\phi_{fl} = 0.11$ was measured[48] relative to the fluorescence of chlorophyll *b* in benzene ($\phi_{fl} = 0.12$), as reported by Weber and Teale (Weber, G.; Teale, F. W. J. *Trans. Faraday Soc.* **1957**, *53*, 646−655). In the same paper, Weber and Teale report the quantum yield $\phi_{fl} = 0.97$ for Rhodamine B in EtOH. As shown later,[41] this value is significantly overestimated.

(50) (a) Sun, X. D.; Li, D. M.; Chen, G. D.; Zhang, J. L. *Dyes Pigm.* **2006**, *71*, 118−122. (b) Lagerberg, J. W. M.; Vanderwal, J.; Charlesworth, P.; Truscott, T. G.; VanDerZee, J.; Schneckenburger, H.; Dubbelman, T. *Free Radical Biol. Med.* **1996**, *21*, 181−188.

(51) Vuorimaa, E.; Lemmetyinen, H.; VanderAuweraer, M.; DeSchryver, F. C. *Thin Solid Films* **1995**, *268*, 114−120.

(52) The separation between the centers of mass of RhB and PtTBP in **5** was estimated as an average over 15 conformations, obtained by means of molecular dynamics, followed by geometry optimization for each conformation (MM+ force field) (see Supporting Information for details).

(53) Mugnier, J.; Pouget, J.; Bourson, J.; Valeur, B. *J. Lumin.* **1985**, *33*, 273−300.

(54) Rehm, D.; Weller, A. *Isr. J. Chem.* **1970**, *8*, 259.

(55) Fischer, A. B.; Bronstein-Bonte, I. *J. Photochem.* **1985**, *30*, 475−485.

(56) The work term was calculated as in ref 54, using the value of 36.7 for the dielectric permeativity of DMF and the distance of 7.5 Å for the separation between PtTBP and RhB in RhB−PtTBP dyads.

(57) (a) Chen, P. L.; Tomov, I. V.; Dvornikov, A. S.; Nakashima, M.; Roach, J. F.; Alabran, D. M.; Rentzepis, P. M. *J. Phys. Chem.* **1996**, *100*, 17507−17512. (b) Knyukshto, V. N.; Shul'ga, A. M.; Sagun, E. I.; Zen'kevich, E. I. *Opt. Spectrosc.* **2006**, *100*, 590−601.

(58) For examples, see: (a) Verhoeven, J. W. *J. Photochem. Photobiol. C: Photochem. Rev.* **2006**, *7*, 40−60. (b) Weiss, E. A.; Ratner, M. A.; Wasielewski, M. R. *J. Phys. Chem. A* **2003**, *107*, 3639−3647. (c) Hviid, L.; Bouwman, W. G.; Paddon-Row, M. N.; van Ramesdonk, H. J.; Verhoeven, J. W.; Brouwer, A. M. *Photochem. Photobiol. Sci.* **2003**, *2*, 995−1001. (d) Kobori, Y.; Yamauchi, S.; Akiyama, K.; Tero-Kubota, S.; Imahori, H.; Fukuzumi, S.; Norris, J. R. *Proc. Natl. Acad. Sci. U.S.A.* **2005**, *102*, 10017−10022.

(59) The value $\Delta r = 3.4$ Å was calculated as the difference between the average end-to-end distances for the linkers consisting of piperazine (for adduct **5**) and piperazine−glycine (for adduct **6**). The distances were averaged over 15 conformations for each linker type (see Supporting Information for details).

(60) Schuler, B.; Lipman, E. A.; Steinbach, P. J.; Kumke, M.; Eaton, W. A. *Proc. Natl. Acad. Sci. U.S.A.* **2005**, *102*, 2754−2759.

(61) (a) Axup, A. W.; Albin, M.; Mayo, S. L.; Crutchley, R. J.; Gray, H. B. *J. Am. Chem. Soc.* **1988**, *110*, 435−439. (b) Cowan, J. A.; Upmacis, R. K.; Beratan, D. N.; Onuchic, J. N.; Gray, H. B. *Ann. N.Y. Acad. Sci.* **1988**, *550*, 68−84. (c) Elias, H.; Chou, M. H.; Winkler, J. R. *J. Am. Chem. Soc.* **1988**, *110*, 429−434. (d) Karas, J. L.; Lieber, C. M.; Gray, H. B. *J. Am. Chem. Soc.* **1988**, *110*, 599−600. (e) Meade, T. J.; Gray, H. B.; Winkler,

J. R. *J. Am. Chem. Soc.* **1989**, *111*, 4353−4356. (f) Therien, M. J.; Selman, M.; Gray, H. B.; Chang, I. J.; Winkler, J. R. *J. Am. Chem. Soc.* **1990**, *112*, 2420−2422.

(62) (a) Steinberg, I. Z.; Harrington, W. F.; Berger, A.; Sela, M.; Katchalski, E. *J. Am. Chem. Soc.* **1960**, *82*, 5263−5279. (b) Engel, J. *Biopolymers* **1966**, *4*, 945. (c) Schimmel, P. R.; Flory, P. J. *Proc. Natl. Acad. Sci. U.S.A.* **1967**, *58*, 52. (d) Stryer, L.; Haugland, R. P.; *Proc. Natl. Acad. Sci. U.S.A.* **1967**, *58*, 719. (e) Deber, C. M.; Bovey, F. A.; Carver, J. P.; Blout, E. R. *J. Am. Chem. Soc.* **1970**, *92*, 6191. (f) Torchia, D. A.; Bovey, F. A. *Macromolecules* **1971**, *4*, 146. (g) Vassilian, A; Wishart, J. F.; van Hemelryck, B.; Schwarz, H.; Isied, S. S. *J. Am. Chem. Soc.* **1990**, *112*, 7278−7286.

(63) Distributions were recovered by the MEM (Livesey, A. K.; Brochon, J. C. *Biophys. J.* **1987**, *52*, 693−706), implemented as a recursive algorithm (Vinogradov, S. A.; Wilson, D. F. *Applied Spectrosc.* **2000**, *54*, 849−855).

(64) The width of a distribution recovered by a regularized inversion method, e.g., the maximum entropy method (MEM), symbolizes the uncertainty in the parameters evaluation and, therefore, is partially related to the noise in the data.[63]

(65) Wagner, B. D.; Ware, W. R. *J. Phys. Chem.* **1990**, *94*, 3489−3494.

(66) For examples, see: (a) Chibisov, A. K.; Slavnova, T. D. *J. Photochem.* **1978**, *8*, 285−297. (b) Arbeloa, I. L.; Ojeda, P. R. *Chem. Phys. Lett.* **1982**, *87*, 556−560. (c) Hoekstra, D.; de Boer, T.; Klappe, K.; Wilschut, J. *Biochemistry* **1984**, *23*, 5675−5681. (d) Arbeloa, F. L.; Ojeda, P. R.; Arbeloa, I. L. *J. Chem. Soc., Faraday Trans. 2* **1988**, *84*, 1903−1912.

(67) A less general formula was used in our previous paper (ref 26), in which we assumed that the 2PA of the "naked" core was negligible compared to that of the antenna. When PtTBPs are being used as cores, eq 3 should be used instead.

(68) Datta-Gupta, N.; Bardos, T. J. *J. Heterocycl. Chem.* **1966**, *3*, 495−502.

(69) Measured in this work.

(70) Barnett, G. H.; Hudson, M. F.; Smith, K. M. *J. Chem. Soc., Perkin Trans. 1* **1975**, 1401−1403.

(71) Meallier, P.; Moullet, M.; Guittonneau, S.; Chabaud, F.; Chevrou, P.; Niemann, C. *Dyes Pigm.* **1998**, *36*, 161−167.